

20 Years of Pulsar Observations with XMM-Newton

Eric Gotthelf (Columbia University)

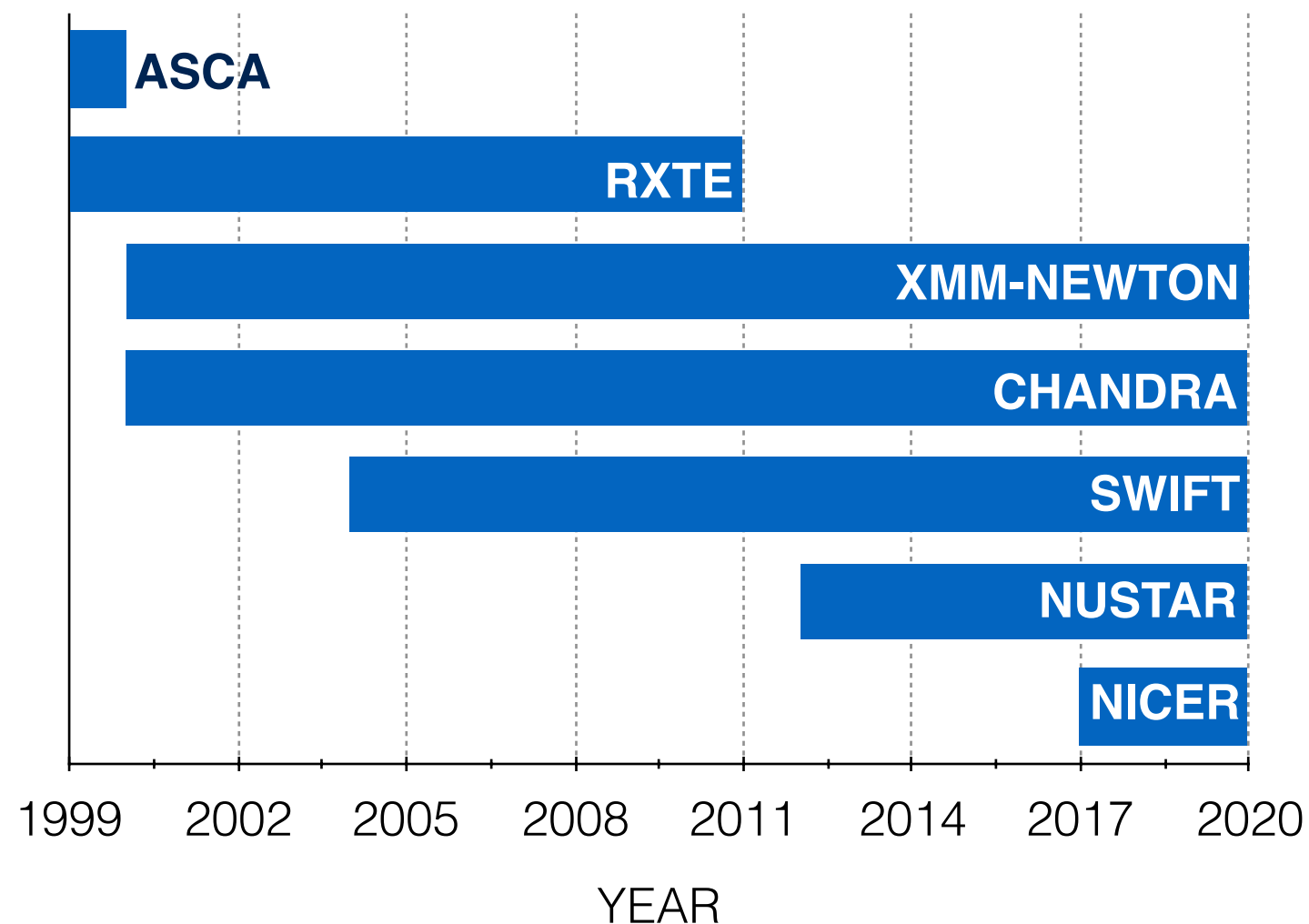
- The X-ray Pulsar Population,
- The XMM-Newton EPIC Instruments For Pulsar Measurements,
- Compilation of XMM-Newton Pulsar Observations,
- A Few of Many, Many Examples of XMM Pulsar Discoveries .

XMM Timeline and Pulsar Science

ASCA was the first broad-band (0.2-12 keV) spectro-imaging mission

XMM fills a critical gap in time for broad-band pulsar studied

Takes the torch from ASCA tempo-imaging...



Pulsar timing torch is now passed to NuStar and NICER,
But joint XMM and Chandra obs. provides a powerful new spectroscopic tool

XMM Observations of Pulsars

XMM-Newton's timing and phase-resolved spectroscopy capabilities is well match for studying the characteristics of pulsars...

The EPIC is the prime instrument for observing pulsars

EPIC pn SmallWindow 5.7 ms resolution (4.3'x4.3' FoV; 71% LiveTime)

EPIC pn Timing 0.03 ms & MOS 1.5 ms (~1D Image; ~100% LiveTime)

XMM EPIC Pulsar timing advantages

Long, uninterrupted observations, large collection area

Sub arcmin PSF, low energy response to 0.2-12 keV

Minimum detectable pulsed fraction $\sim f_p(\text{min}) \sim \sqrt{2S/N}$,

N = total counts, S =signal power (FFT, Z^2_n)

$f_p(\text{min})$ is increased by background counts N_b , as $(1+N_b/N_s)$

Background included all unpulsed detected counts

The X-ray Pulsar Population

- RPPs: Rotation-Powered Pulsars (young/high \dot{E} , Crab/Vela)
- XINSs: X-ray Isolated Neutron Stars (Magnificent Seven)
- CCOs: Central Compact Object in SNR (3 Anti-magnetars)
- Magnetars: Soft Gamma-ray Repeaters (SGRs),
Anomalous X-ray Pulsars (AXPs),
Transient AXPs (TAXPs)
- Binaries: Older pulsars in non-accreting binaries systems,
- MSPs: Millisecond Pulsars ($\sim < 5\text{ms}$; old, recycled pulsars)

X-ray pulsars represent the population of young NSs, powered by:

Hot, residual thermal X-rays, $kT \sim 0.5\text{ keV}$ (localized hot spots)

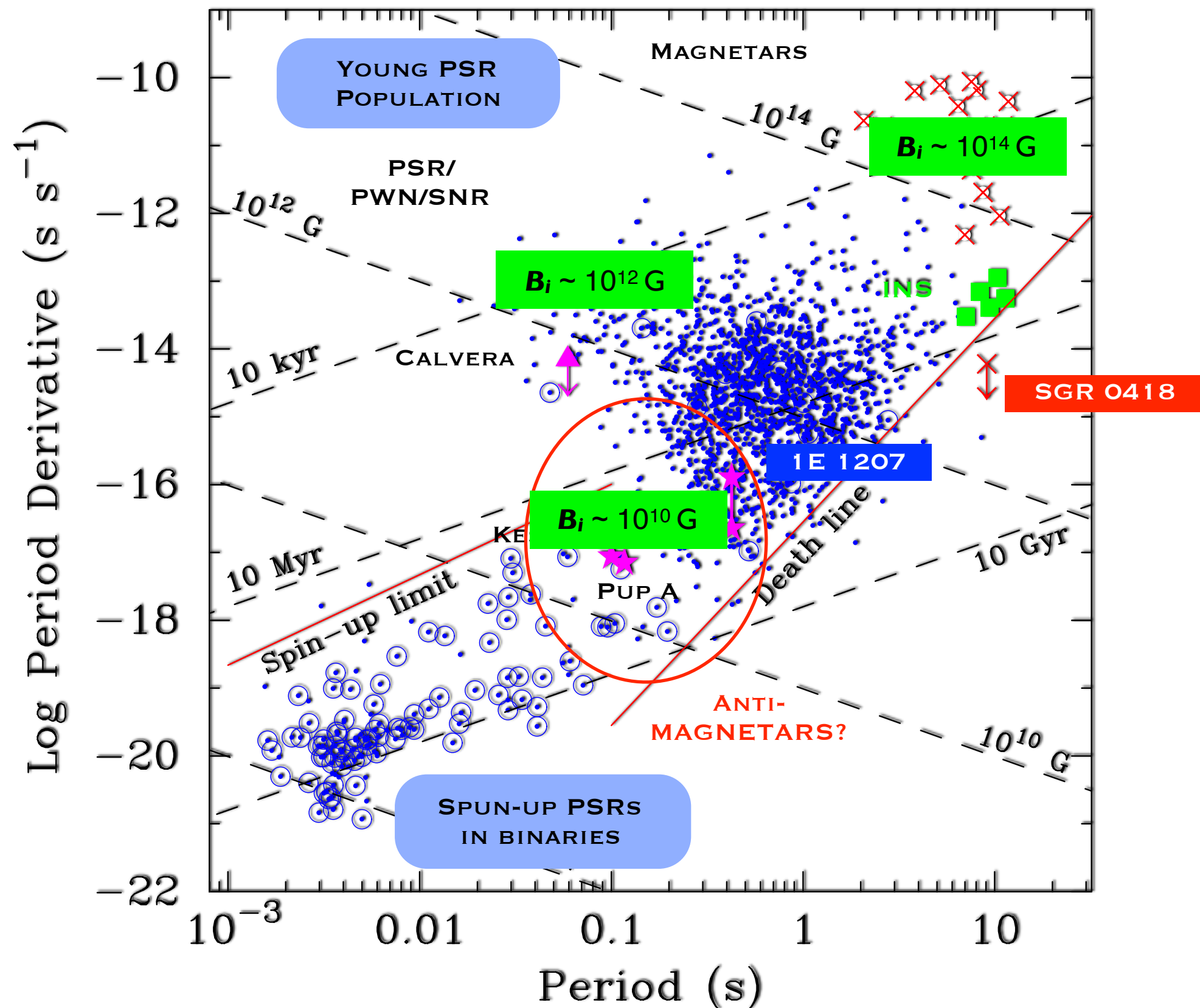
Non-thermal photospheric, $L_x \sim \dot{E}^a$ (generating a PWN)

Magnetic field decay (Ohmic losses)

In terms of birth rate, these classes of NSs have similar numbers

XMM-Newton's leaves a rich legacy of pulsar science, ongoing...

Pulsars on the P-Pdot diagram



XMM Exposure Time for Pulsars

XINSs, CCOs, Magnetars, RPPs, Binaries, MSPs
Total of ~39 Ms (>3 yrs of XMM obs.)

XINS	XMM (ks)
RX J0420.0-5022	254
RX J0720.4-3125	787
RX J0806.4-4123	237
RX J1308.6+2127	204
RX J1605.3+3249	662
RX J1856.6-3754	2,624
RX J2143.0+0654	171
7 Total:	4,937

CCO Pulsar	SNR	XMM (ks)
1E 1207.4-5209	PKS 1209-51/52	974
PSR J0821-4300	Puppis A	806
PSR J1852+0040	Kes 79	525
	3 Total:	2,305

Method: Corr. ATNF pulsars with XMM Obs.
Exclude serendipitous match > 5'

Magnetar	SNR	XMM (ks)
CXOU J010043.1-721134		347
4U 0142+61		150
SGR 0418+5729		540
SGR 0501+4516	SNR G160.9+2.6	215
SGR 0526-66	SNR N49	117
1E 1048.1-5937	GSH 288.3-0.5-28?	394
1E 1547.0-5408	SNR G327.24-0.13	185
CXOU J162244.8-495054	SNR G333.9+0.0	210
SGR 1627-41	CTB 33	395
CXO J164710.2-455216	Westerlund 1	279
RXS J170849.0-400910		100
CXOU J171405.7-381031	CTB 37B	192
SGR J1745-29	Galactic Center	3,232
SGR 1806-20	W31	496
XTE J1810-197		871
SGR J1822-1606	M17	139
SGR 1833-0832		77
CXOU J183452.1-084556	W41	229
1E 1841-045	Kes 73	97
AX J1845-0258		170
3XMM J185246.6+003317		525
SGR 1900+14	SNR G42.8+0.6	158
SGR 1935+2154	SNR G57.2+0.8	253
1E 2259+586	CTB 109	306
	24 Total:	9,698

Pulsars in Non-accreting Binary Systems

Nearly all are MSPs.

Nearly all radio and/or
Gamma-ray pulsars

Few detected
as X-ray pulsars

MSPs with X-ray Detected Pulsations

Pulsar	Assoc.	XMM (ks)
J0034-0534	2FGL_J0034.4-0534	38
J0218+4232	2FGL_J0218.1+4233	41
J0337+1715	*	19
J0437-4715	Bright MSP (XMM Pulsar)	198
J0514-4002A	NGC 1851	23
J0613-0200	2FGL_J0613.8-0200	73
J0614-3329	2FGL_J0614.1-3329	14
J0636+5129	*	18
J0737-3039A	Double NS binary (XMM Pulsar)	661
J0751+1807	2FGL_J0751.1+1809	38
J0952-0607	*	71
J1012+5307	*	38
J1017-7156	*	13
J1023+0038	AY_Sex (TMSP)	903
J1125-5825	2FGL_J1125.0-5821	22
J1227-4853	XSS J12270-4859 (TMSP)	152
B1259-63	*	275
J1311-3430	2FGL_J1311.7-3429	208
J1400-1431	3FGL_J1400	40
J1446-4701	2FGL_J1446.8-4701	62
J1513-2550	3FGL_J1513.4-2549	25
B1534+12	Double NS binary	130
J1543-5149	*	9
J1600-3053	2FGL_J1600.7-3053	31
J1614-2230	2FGL_J1614.5-2230	90
J1622-0315	3FGL_J1622.9-0312	22
J1638-4725	*	99
B1639+36B	M13	139
J1643-1224	*	24
J1719-1438	*	15
J1723-2837	2MASS_J17232318-2837571	62

Pulsar	Assoc.	XMM (ks)
J1731-1847		39
J1737-0811	*	16
J1744-3922	*	6
J1748-2021B	NGC6440	194
B1744-24A	Ter5	80
J1750-3703A	NGC6441	195
J1750-3703B	NGC6441	195
J1810+1744	3FGL_J1810.5+1743	82
J1824-2452C	M 28	98
J1836-2354A	M 22	41
J1853+1303	*	31
B1855+09	*	13
J1909-3744	*	51
J1911-1114	*	68
J1946+2052	*	22
J1946-5403	3FGL_J1946.4-5403	20
B1957+20	2FGL_J1959.5+2047	31
J2017-1614	3FGL_J2017.6-1616	25
J2032+4127	MT91_213,Cygnus_OB2	175
J2051-0827	*	48
J2052+1218	3FGL_J2052.7+1217	24
J2115+5448	3FGL_J2114.9+5448	21
J2129-0429	2FGL_J2129.8-0428	80
B2127+11C	M 15	97
J2129-5721	*	59
J2214+3000	2FGL_J2214.7+3000	86
J2215+5135	3FGL_J2215.6+5134	54
J2241-5236	2FGL_J2241.7-5236	51
J2302+4442	2FGL_J2302.7+4443	25
J2339-0533	0FGL_J2339.8-0530	181
61 Total:		5,600

MSP	Assoc.	XMM (ks)
J0030+0451		162
J0218+4232		42
J0437-4715		199
J1024-0719		71
B1821-24A	M 28 GC	99
B1937+21		67
B1957+20		32
J2124-3358		137
8 Total:		809

Rotation Powered Pulsars (not in globular clusters)

Pulsar	Association	XMM (ks)
J0007+7303	CTA1	169
J0030+0451	2FGL_J0030.4+0450	162
J0108-1431	*	135
B0114+58	*	10
B0136+57	*	9
B0154+61	*	33
J0205+6449	3C58	264
J0250+5854	*	133
J0357+3205	2FGL_J0357.8+3205	121
B0355+54	PWN	30
B0450-18	*	38
J0519-6932	RX_J0520.5-6932	50
B0531+21	Crab Nebula	1460
J0537-6910	N157B	48
J0538+2817	S147	18
B0540-69	SNR 0540-693	460
B0540+23	*	26
B0611+22	*	44
B0628-28	RX_J0630.8-2834	49
J0631+0646	3FGL_J0631.6+0644	22
J0631+1036	2FGL_J0631.5+1035	25
J0633+0632	2FGL_J0633.7+0633	94
J0633+1746	Geminga	328
J0635+0533	SAX	88
J0645+5158	*	37
B0656+14	Monogram Ring	171
J0711-6830	*	16
J0726-2612	1RXS_J072559.8-261229	109
B0740-28	2FGL_J0742.4-2821	22

Pulsar	Association	XMM (ks)
B0743-53	*	23
B0823+26	*	239
B0826-34	*	56
B0833-45	Vela Nebula	1639
B0834+06	*	72
J0855-4644	RX_J0852.0-4622(?)	56
B0906-49	*	10
B0919+06	*]	42
B0940-55	*	23
J0945-4833	*	22
B0943+10	*	650
B0950+08	*	95
J0954-5430	*	19
J0957-5432	*	20
J1000-5149	*	11
B1001-47	*	19
J1024-0719	2MASS_10243869-0719100	71
B1046-58	2FGL_J1048.2-5831	32
B1055-52	2FGL_J1057.9-5226	261
J1101-6101	MSH 11-61A	86
J1119-6127	SNR G292.2-0.5	297
J1124-5916	SNR G292.0+1.8	118
B1133+16	*	147
J1154-6250	*	62
B1221-63	*	7
B1338-62	SNR G308.8-0.1	70
J1357-6429	PWN	100
J1412+7922	Calvera	59
J1418-6058	HESS_	161

Pulsar	Association	XMM (ks)
J1420-6048	HESS_J	166
J1437-5959	SNR G315.9-0.0	135
B1449-64	*	7
J1455-59	*	7
J1459-6053	2FGL_J1459.4-6054	106
J1509-5850	2FGL_J1509.6-5850	131
B1509-58	Cir SNR G320.4-1.2	82
B0833-45		
J1549-4848	*	96
J1613-5211	*	52
J1614-5144	*	74
J1617-5055	*	282
J1624-4041	3FGL_J1624.2-4041	32
B1634-45	*	12
J1640-4631	SNR G338.3-0.0	24
B1643-43	SNR G341.2+0.9(?)	28
J1651-4519	*	43
J1705-1903	*	8
B1702-19	*	8
J1705-4108	*	8
B1703-40	*	18
B1706-44	SNR G343.1-2.3(?)	87
J1713-3949	*	329
J1718-3825	2FGL_J1718.3-3827_HESS_J1718.3-3827	25
B1719-37	*	8
J1725-0732	*	19
J1730-2304	*	32
B1727-33	*	15
B1727-47	RCW_114	38

Pulsar	Association	XMM (ks)
J1734-3333	*	205
J1740+1000	*	731
B1737-30	*	9
J1741-2054	2FGL_J1741.9-2054	71
J1744-7619	3FGL_J1744.1-7619	26
B1742-30	*	9
J1747-2809	SNR G0.9+0.1	53
J1747-2958	PWN G359.23-0.82	43
J1755-0903	*	9
B1754-24	*	16
B1757-24	SNR G5.4-1.2	9
J1808-2701	*	22
J1809-2332	2FGL_J1809.8-2332	217
J1811-1925	SNR G11.2-0.3	29
J1813-1246	2FGL_J1813.4-1246	109
J1813-1749	SNR 12.8-0.0	158
J1814-1744	*	7
B1818-04	*	34
B1822-09	*	228
J1826-1256	2FGL_J1826.1-1256	141
B1823-13	PWN G18.0-0.7	58
J1833-1034	SNR G21.5-0.9	78
J1838-0537	3FGL_J1838.9-0537	45
J1838-0655	HESS J1837-069	63
J1844-0256	*	171
J1846-0258	Kes 75 SNR	54
J1847-0130	*	19
B1845-19	*	66
J1849-0001	IGR_18490-	66

Pulsar	Association	XMM (ks)
B1853+01	W44 SNR	461
J1856+0245	HESS J1857+026	56
J1901+0254	*	17
B1916+14	*	33
B1919+21	*	20
J1926-1314	*	79
J1930+1852	SNR G54.1+0.3	164
B1929+10	*	258
B1937+21	*	67
B1944+17	*	27
B1951+32	CTB 80 SNR	55
J1957+5033	2FGL_J1957.9+5033	1
J2021+3651	AGL_J2020.5+3653	206
J2021+4026	SNR G78.2+	277
J2022+3842	SNR G76.9+1	119
J2043+2740	2FGL_J2043.7+2743	17
J2055+2539	2FGL_J2055.8+2539	179
J2124-3358	2FGL_J2124.6-3357	137
J2144-3933	*	42
B2224+65	Guitar Nebula	76
J2229+6114	SNR G106.6+2.9	37
B2334+61	SNR G114.3+0.3	48
	139 Total:	15,632

XMM Observations of Isolated Neutron Stars

X-ray Isolated Neutron Stars (The Magnificent Seven)

XINSs (XDINSs) are nearby isolated, cooling NS ($kT \sim 40 - 110$ eV; $F_x/F_{optical} > 10^4$)

- All 7 ROSAT XINSs well-observed by XMM (5 Ms),
- XMM discovered 5 as pulsars, $P \sim 3 - 17$ s, $f_p \sim 4 - 18\%$,
- Spin-down $\tau \sim 1 - 2$ Myr, $B \sim 10^{13}$ G, $\dot{E} \sim 5 \times 10^{30}$ erg/s.

XINS	XMM (ks)
RX J0420.0-5022	254
RX J0720.4-3125	787
RX J0806.4-4123	237
RX J1308.6+2127	204
RX J1605.3+3249 (no PSR)	662
RX J1856.6-3754	2,624
RX J2143.0+0654	171
7 Total:	4,937

XMM Results

- Spectral absorption features ($\sim 0.2 - 0.8$ keV) for 6 XINSs,
- Pulse phase dependence of these features (e.g., Haberl et al. 2003),
- They can vary over long-term (e.g., van Kerwijk et al. 2004)
- Interpreted as cyclotron lines implies high magnetic fields ($B \sim 10^{13}$ G),
- This field strength is consistent with those inferred from spin-down down.

Big Picture

Could XDINSs be evolved magnetars, born from similar populations of massive stars?

XMM-Newton Discovery of 7s Pulsations in the Isolated Neutron Star RX J1856.5-3754

(Tiengo & Mereghetti 2007)

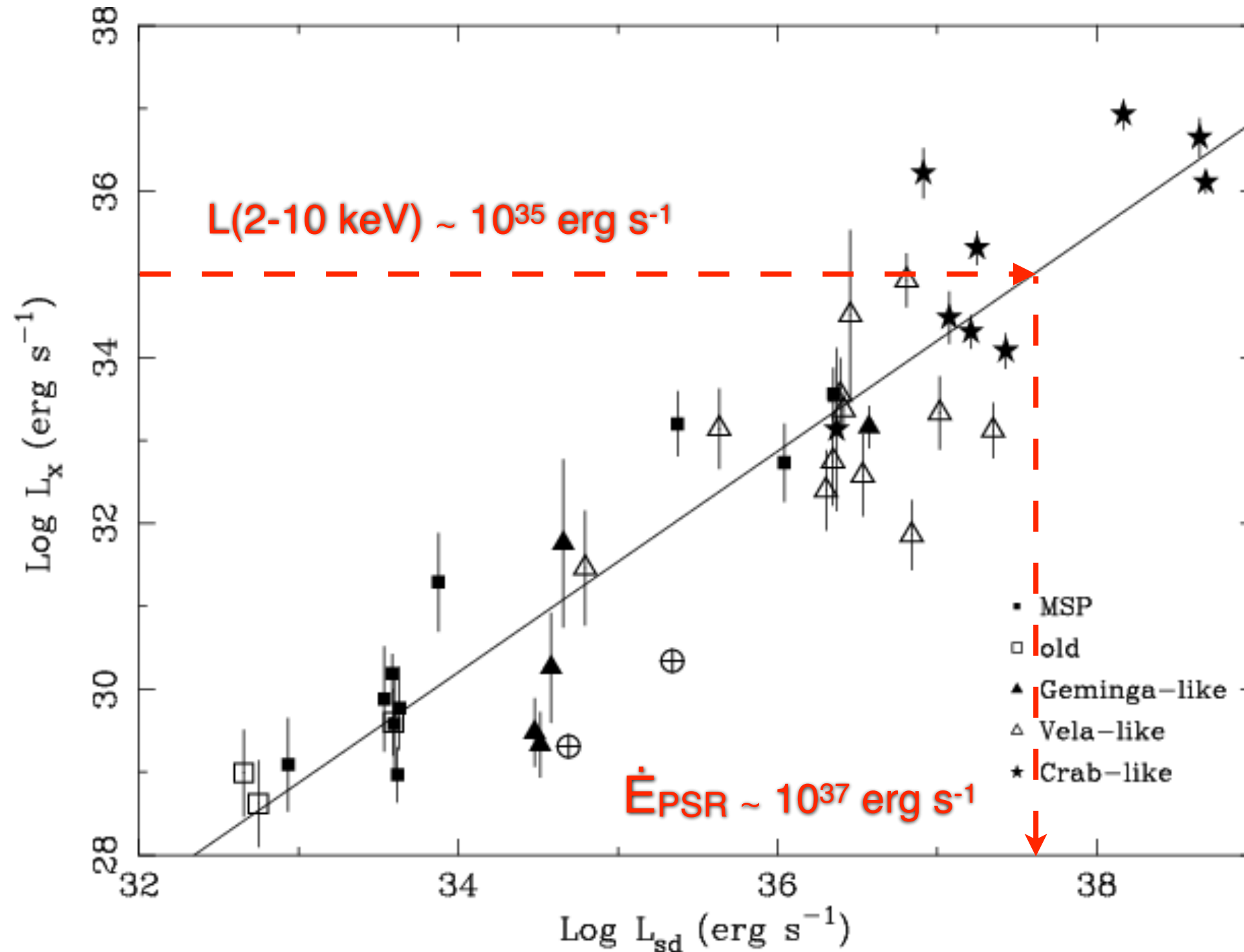
RX J1856.5–3754 brightest XINSs, $d=117$ pc, but the weakest signal ($\sim 1.2\%$),
Monitored extensively with XMM, almost twice a year from 2002, totaling 2.6 Ms.
Purely thermal spectrum with $kT^\infty = 38.9$ eV and $kT^\infty = 62.4$ eV,
Inferred timing properties, $\tau = 3.7$ Myr, $\mathbf{B} = 1.5 \times 10^{13}$ G, $\dot{\mathbf{E}} = 3.3 \times 10^{30}$ erg/s,
Search for variations of its spectral parameters, none found.

Ongoing XMM and Optical Studies

Apply NS atmosphere models for the surface emission to constrain EoS (M-R rel.),
Suggests close alignment b/w the observational geometry and magnetic axis,
Considering evidence for vacuum birefringence,
Stellar origin, evidence for Upper Scorpius OB association as parental stellar cluster.

XMM Observations of Rotation-powered Pulsars

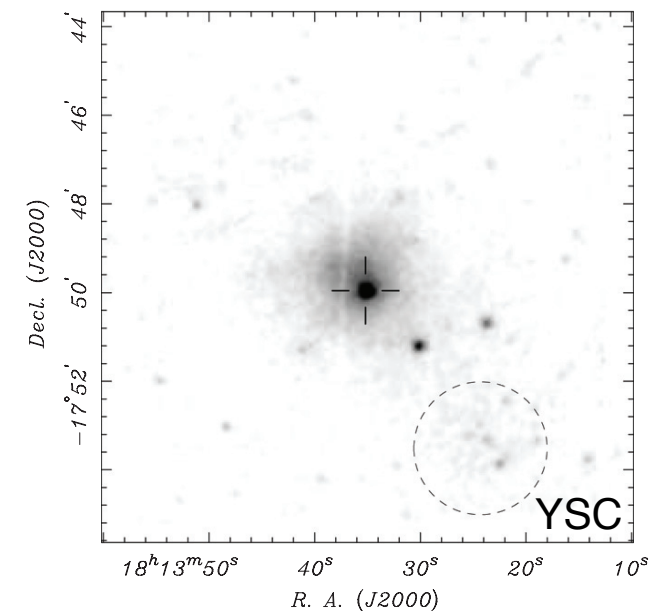
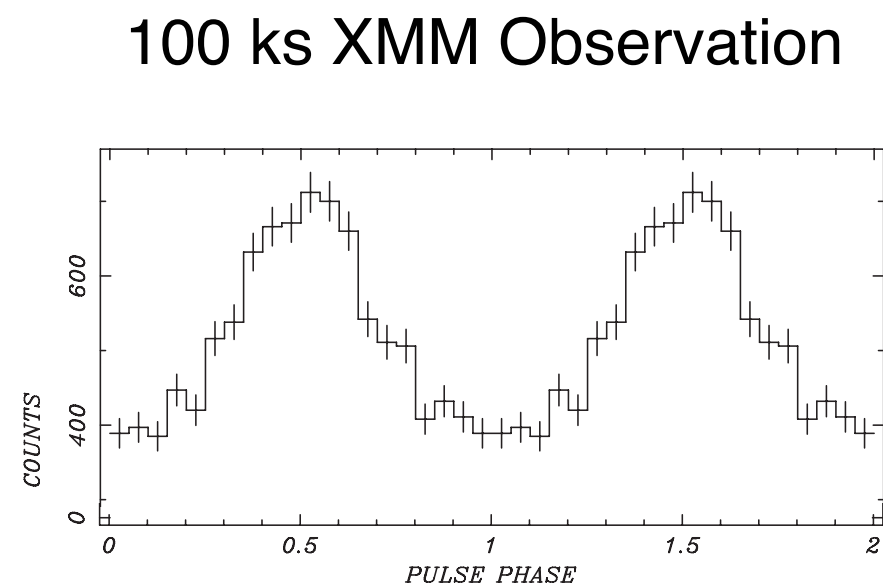
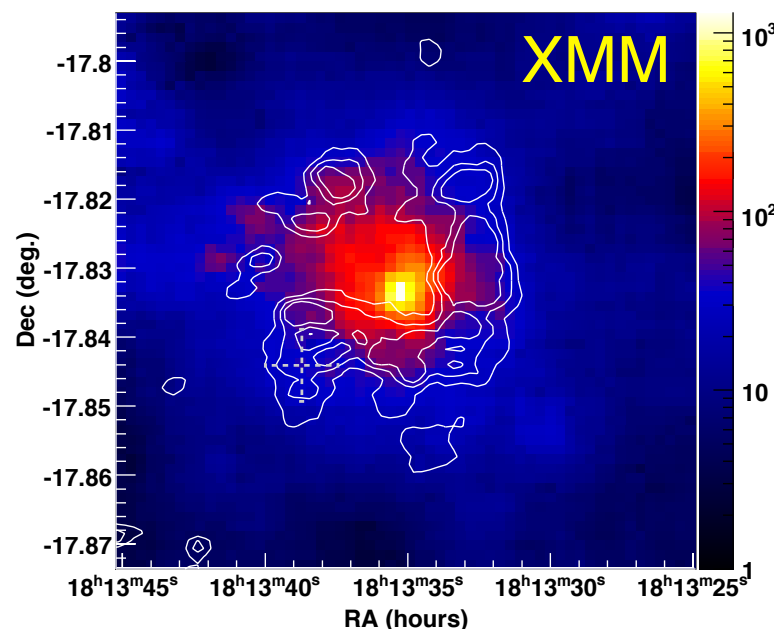
$L(2-10 \text{ keV})$ vs. \dot{E}_{PSR} from Possenti et al. 2002



Discovery of a Highly Energetic X-ray Pulsar Powering HESS J1813–178 in the Young SNR G12.82–0.02

(Gotthelf & Halpern 2009)

PSR J1813-1749 ($P = 44$ ms) is the 2nd most energetic pulsar in the Galaxy,
Spin-down luminosity $\dot{E} = 5.6 \times 10^{37}$ erg/s, age $\tau = 5.6$ kyr, $B = 2.4 \times 10^{12}$ G,
Nearby young stellar cluster (YSC) is possible the birthplace of the pulsar progenitor,
Provides a reservoir of seed photons for inverse Compton scattering to TeV energies.
If associated with the YSC young stellar cluster (d=4.7 kpc), the spin-down conversion
eff. $L_x/\dot{E} = \approx 0.07\%$ for the >200 GeV, enough to power HESS J1813–178

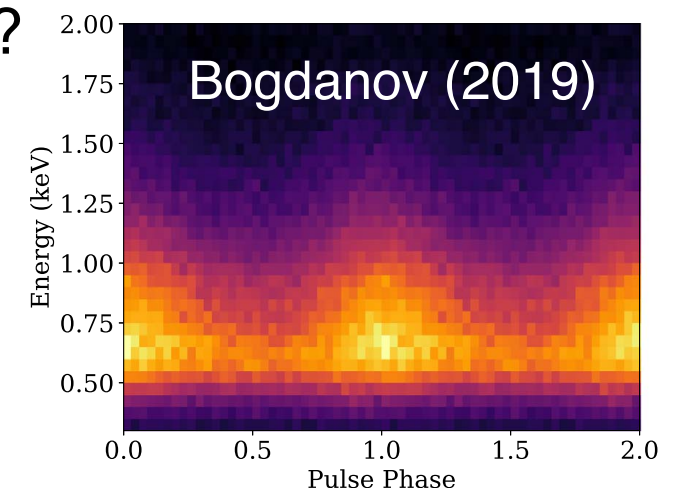


Discovery of 59 ms Pulsations from 1RXS J141256.0+792204 (Calvera)

(Zane et al. 2011)

A mysterious ROSAT object (Rutledge et al. 2007)

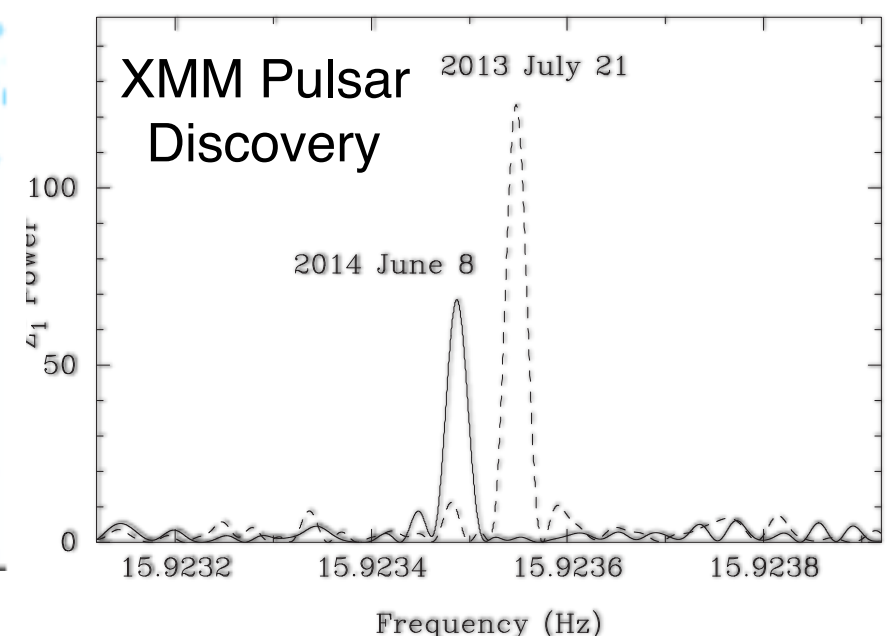
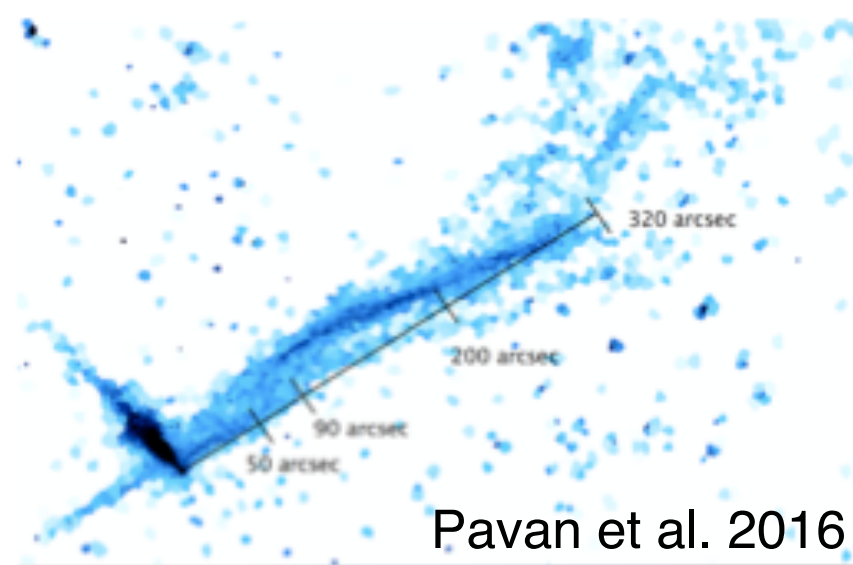
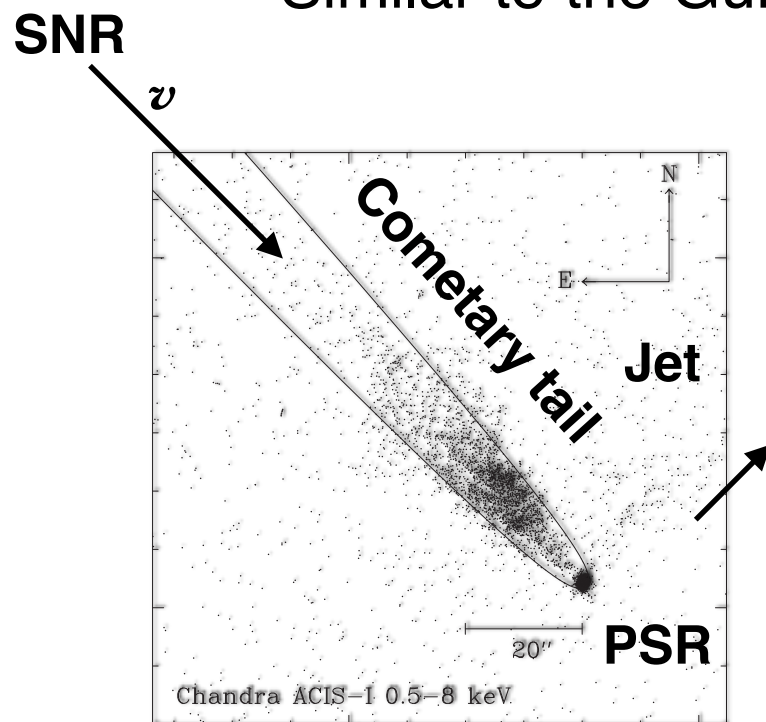
- High B-field INS whose properties does not allow easy classification,
- Soft thermal spectrum ($kT = 0.2$ keV) similar to MSPs & INSs,
- Inferred distance above the Galactic plane implied extreme velocity
- Evidence was found for an absorption feature at 0.65 keV
- PSR J1412+7922 is a XMM discovered 59.2 ms radio-quiet gamma-ray pulsar
- Spin-down luminosity $\dot{E} = 6.3 \times 10^{35}$ erg/s, age $\tau = 285$ kyr, $B = 4.5 \times 10^{11}$ G,
- Strongly energy-dependent pulse fraction
- Rotation-powered? Orphaned CCO? Mildly Recycled Pulsar?



Discovery of X-ray Pulsations from the *INTEGRAL* source *IGR* J11014-6103

(Halpern et al. 2014)

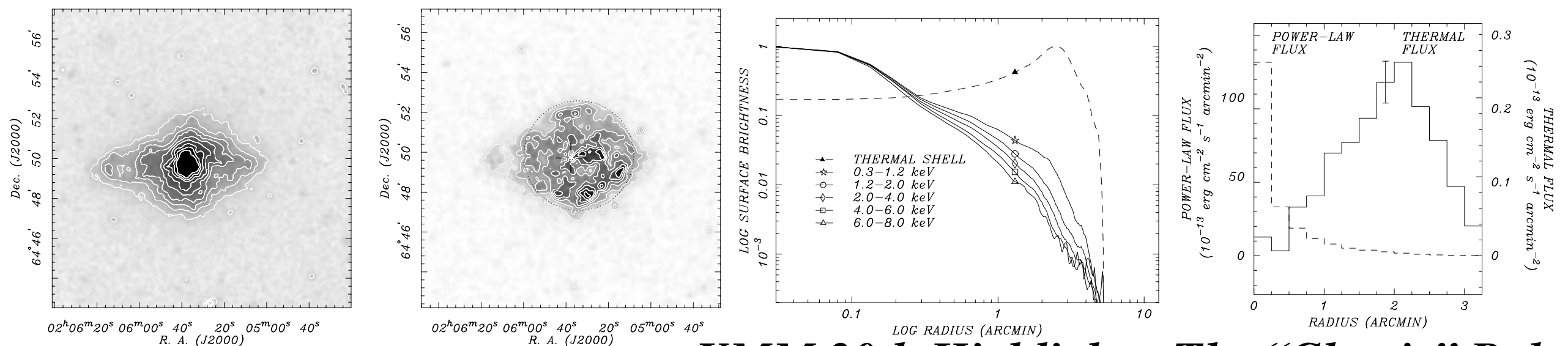
- PSR J1101-6101 is young, radio-quiet $P = 62.8$ ms X-ray pulsar
- Spin-down luminosity $\dot{E} = 1.4 \times 10^{36}$ erg/s, age $\tau = 116$ kyr, $B = 7.4 \times 10^{11}$ G,
- Least energetic of the 15 RPP *INTEGRAL* pulsars
- At 12' from young SNR MSH 11-61A, associated?
- If so, highest velocity pulsar known ~ 1000 km/s
- Similar to the Guitar Nebula + PSR J224+64



A Shell of Thermal X-ray Emission Surrounding the Young Crab-like Remnant 3C 58

(Gotthelf, Helfand & Newburgh 2007)

3C 58 is the bright pulsar wind nebula surrounding PSR J0205+6449,
 Known as a twin of the Crab Nebula, 3C 58 also seemed to lack a thermal SNR,
 Using deep XMM imaging-spectroscopy the thermal shell is finally revealed,
 Strong emission lines of Ne ix He-like transition are detected,
 These require an overabundance of 3 x (Ne/Ne_⊙) in the Raymond-Smith plasma model,
 The best-fit temperature ***kT*** = 0.23 keV is found to be essentially independent of radius,
 The L_x for the 3C 58 shell is >10x the upper limit on a similar Crab Nebula shell,
 We predict t_{SN}=3700 yr based on the shell offset from the pulsar location (Crab vel.).



XMM 20th Highlights: The “Classic” Pulsars

XMM Observations of Magnetars

Magnetar	SNR	XMM (ks)
CXOU J010043.1-721134		347
4U 0142+61		150
SGR 0418+5729		540
SGR 0501+4516	SNR G160.9+2.6	215
SGR 0526-66	SNR N49	117
1E 1048.1-5937	GSH 288.3-0.5-28?	394
1E 1547.0-5408	SNR G327.24-0.13	185
CXOU J162244.8-495054	SNR G333.9+0.0	210
SGR 1627-41	CTB 33	395
CXO J164710.2-455216	Westerlund 1	279
RXS J170849.0-400910		100
CXOU J171405.7-381031	CTB 37B	192
SGR J1745-29	Galactic Center	3,232
SGR 1806-20	W31	496
XTE J1810-197		871
SGR J1822-1606	M17	139
SGR 1833-0832		77
CXOU J183452.1-084556	W41	229
1E 1841-045	Kes 73	97
AX J1845-0258		170
3XMM J185246.6+003317		525
SGR 1900+14	SNR G42.8+0.6	158
SGR 1935+2154	SNR G57.2+0.8	253
1E 2259+586	CTB 109	306
	24 Total:	9,698

The Magnetars

XMM has observed all magnetars, many contributing to their spectral and timing studies, Especially for the new, outbursting magnetars, and ones that are faint in quiescence.

XMM + NuSTAR allows detailed studies of the broad-band, phase-resolved spectrum

The last 2 decades has seen the synthesis of the SGRs, AXPs, TAXPs, as magnetars,

Discovery of a few lower field pulsar with magnetar-like behavior ($\sim 10^{13}$ G),

Even an RPP has exhibited magnetar burst and flares (PSR J1846-0258 in SNR Kes 75)

XMM phase resolved spectroscopy of SGR 0418+5729 reveals shifting absorption line.

Highly variable spin-down (2x), erratic flux, complex energy-dependent pulse profiles,

Reoccurring short soft gamma-ray bursts (“Soft Gamma-ray Repeaters”),

Persistent X-rays, ms bursts, short flares, and outbursts lasting years,

Radio emission from magnetars, sporadic, associated with X-ray outbursts,

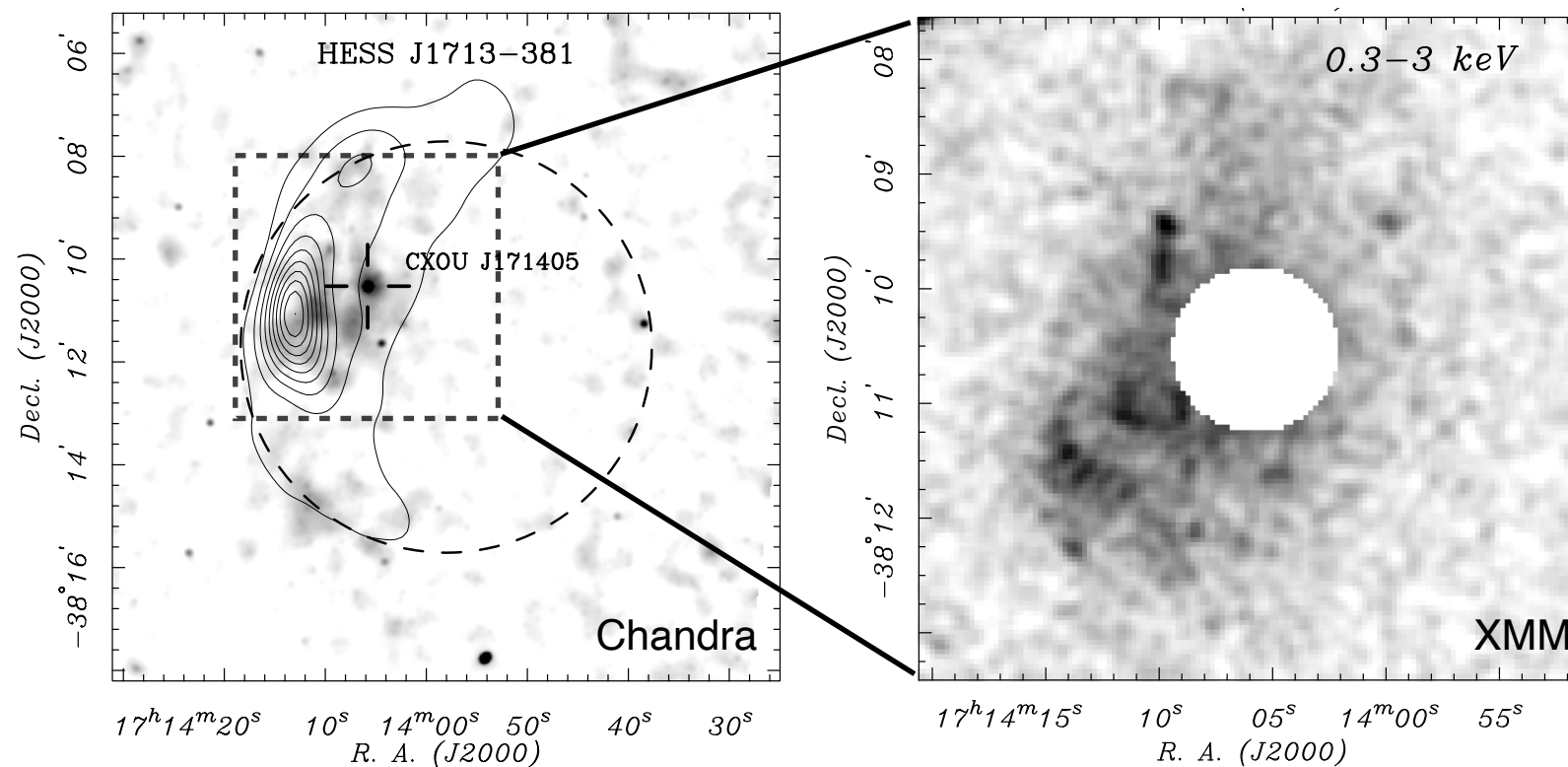
X-ray spectra modeled by a 2T BB model ($kT \sim 0.3, 0.6$ keV) or a BB+PL ($kT \sim 0.3, \Gamma \sim 4$),

X-ray spectrum above 10 keV has an additional, flatter power-law ($\Gamma \sim 1$)

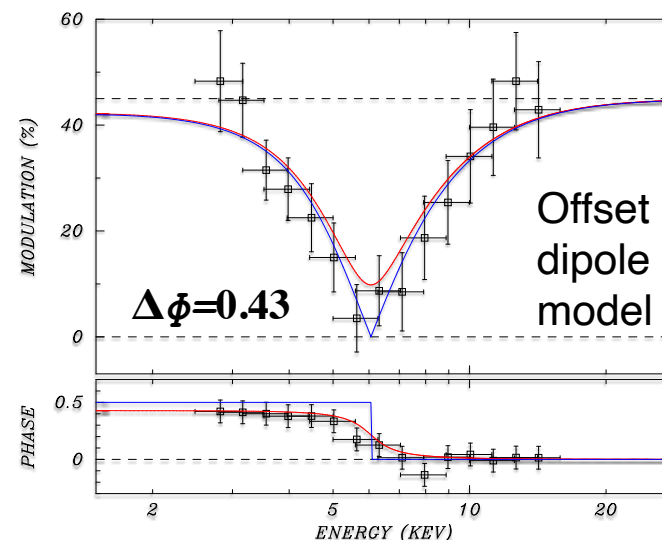
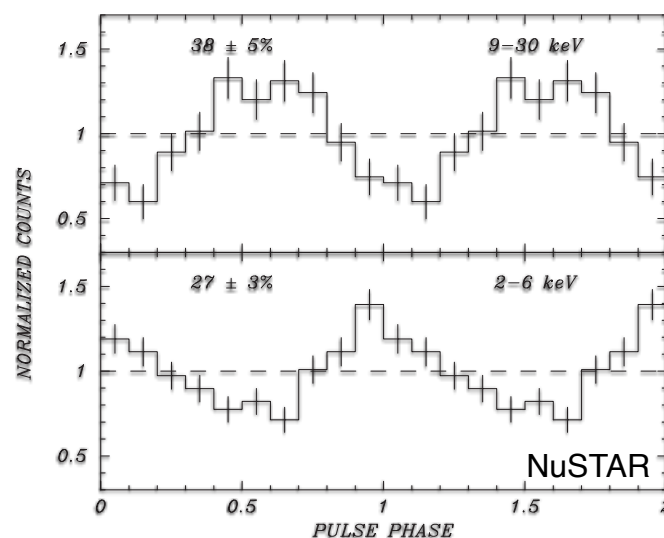
A magnetar in SNR CTB 37B coincident with HESS J1713-381

(Halpern & Gotthelf 2010, 2011; Gotthelf et al. 2019)

Youngest ($\tau=1$ kyr), most energetic (4.2×10^{34} erg s $^{-1}$) magnetar (5×10^{14} G)



- Central 3.82 s magnetar,
- 2nd assoc. with a PWN,
- Variable spin-down (2x),
- Unlike SGRs, no bursts, yet.
- CBB + PL, antipodal



- Evidence for an X-ray PWN,
- (Similar to Swift J1834.9–0846 / SNR (W41) / HESS J1834–097),
- TeV from relic electrons from a dissipated PWN?

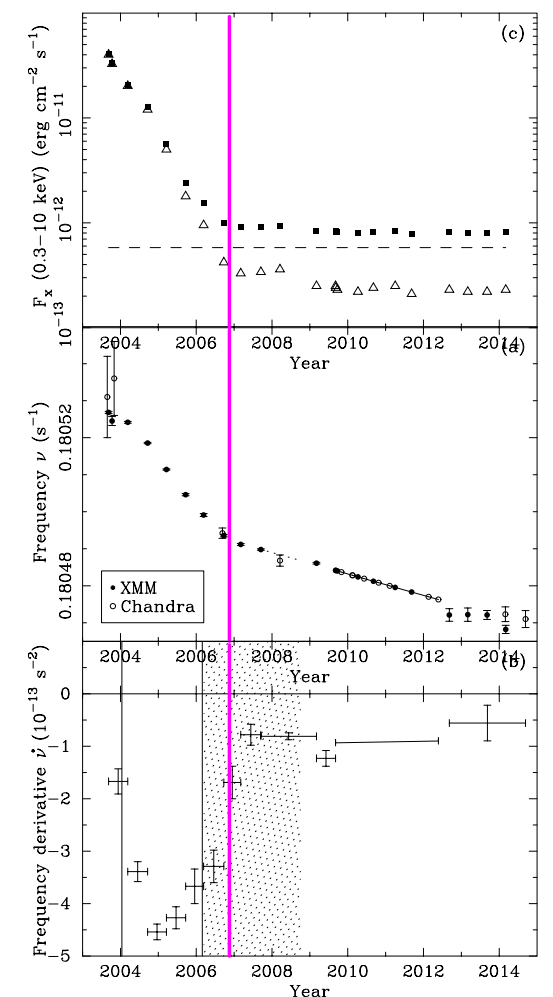
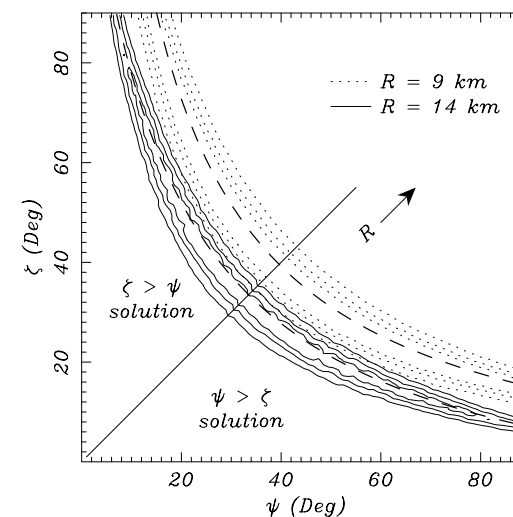
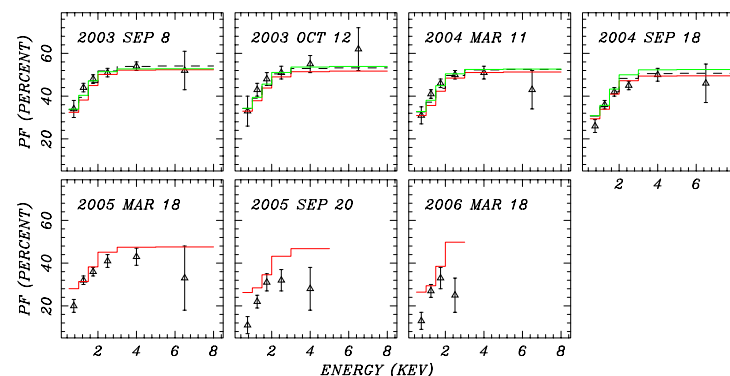
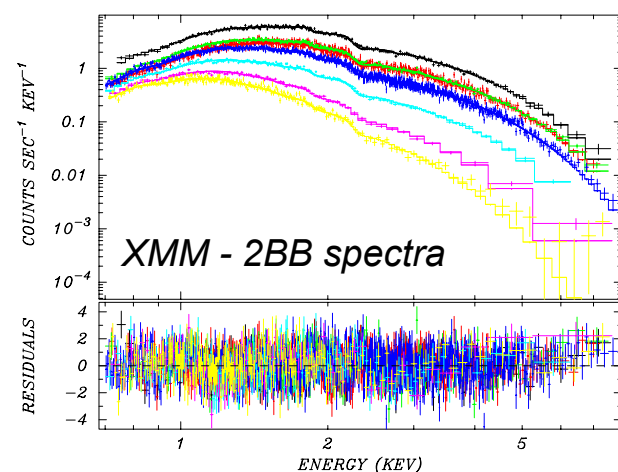
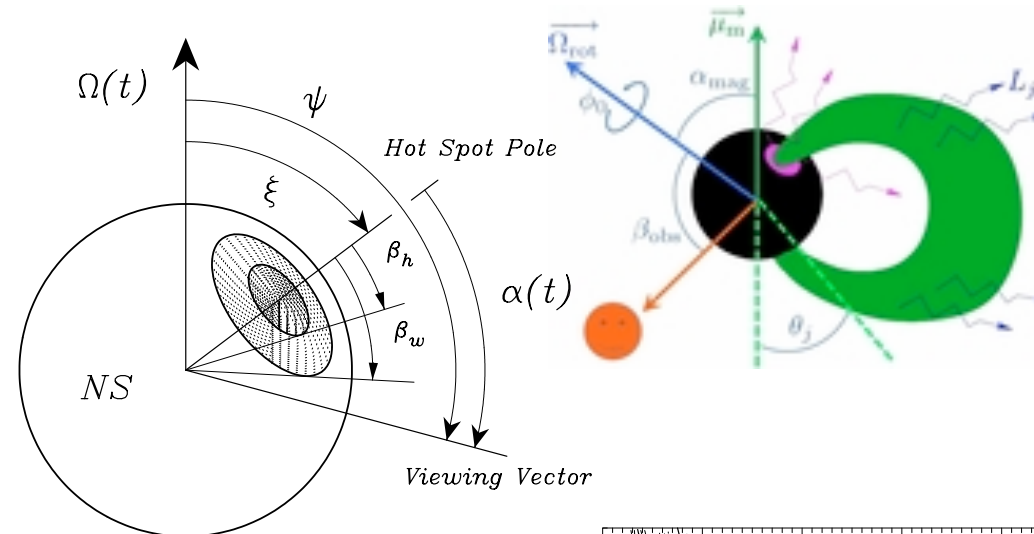
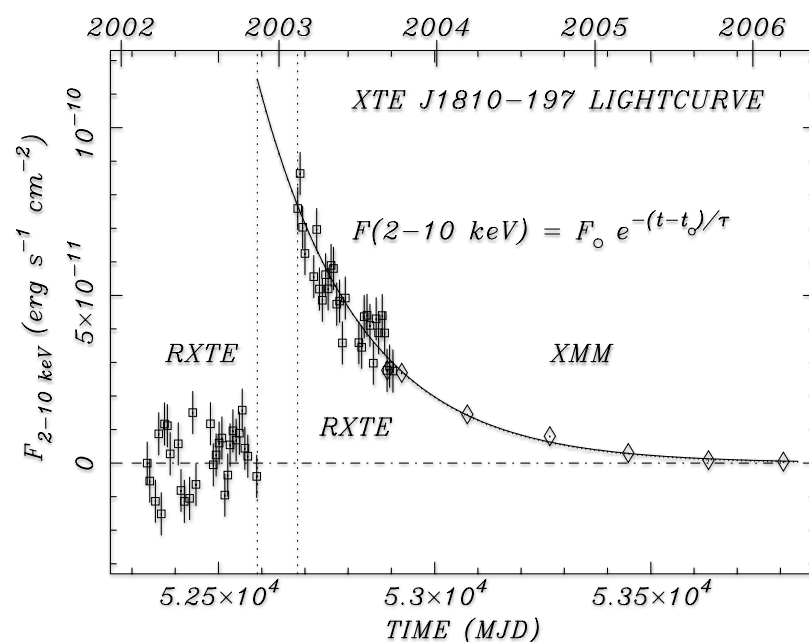
The Anatomy of a Magnetar: XMM Monitoring of the Transient Anomalous X-ray Pulsar XTE J1810 197

(Gotthelf & Halpern 2007)

First transient magnetar discovered (Ibrahim et al. 2004);

First radio magnetar discovered (Halpern et al. 2005),

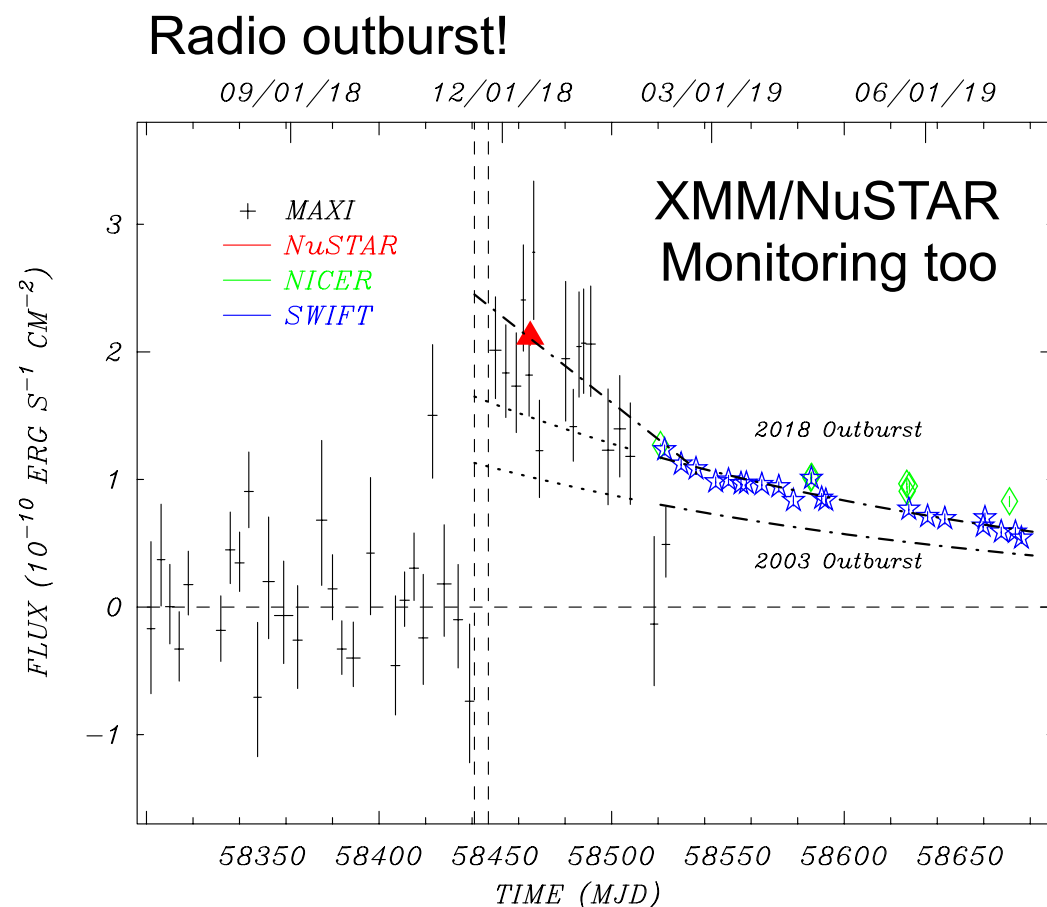
Inspired Beloborodov (2009) theory of untwisting magnetospheres of NSs.



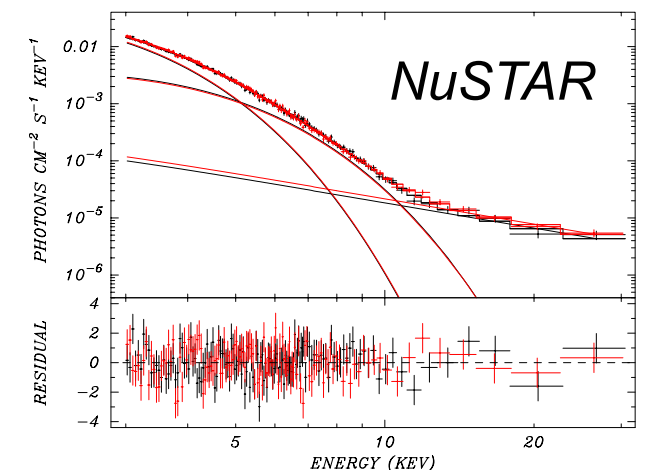
The 2018 X-Ray and Radio Outburst of Magnetar XTE J1810-197

(Gotthelf et al. 2019)

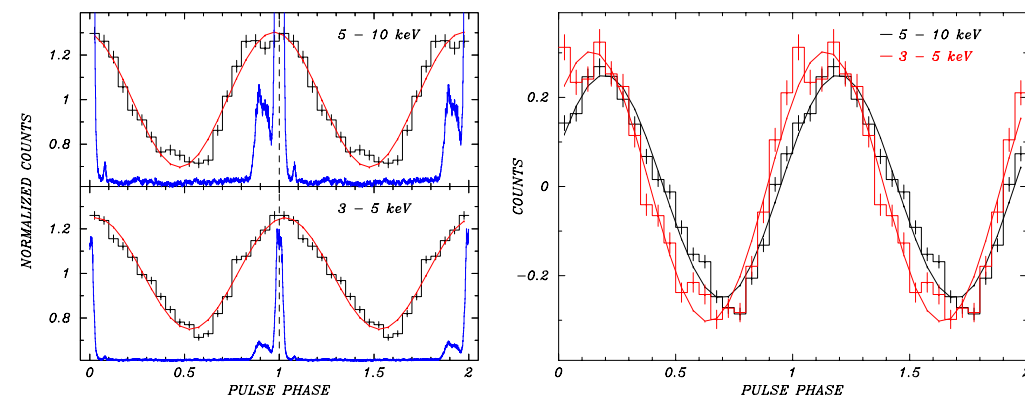
Reawakening: The Dec 2018 radio (Lyne 2018)) / X-ray outburst of XTE J1810-197,
The magnetar underwent a new X-ray outburst, more energetic, caught much earlier,
Following temporal evolution to test untwisting B-field bundle theory,
Campaign using XMM / NuSTAR / NICER underway.



Hard X-ray
non-thermal
component



Energy dependent pulse phase offset



XMM 20th Highlights: The Magnetars

XMM Observations of Millisecond Pulsars

Millisecond Pulsars (MSPs):

These rapidly spinning NSs are theorized to originate in LMXB, where they are spun up (recycled) to millisecond periods by accretion, and emerge as rotation-powered, radio MSPs when the accretion stops.

For the first time, switching between rotation-powered and accretion-powered states has been observed in a pulsar system, supplying the missing link between the radio MSPs and their LMXB progenitors, and providing strong support for the recycling theory. I

In March 2013, the INTEGRAL satellite detected a bright transient source IGR J18245-2452 in the globular cluster M28. Follow-up observations with XMM (Papitto et al. 2013) using the EPIC pn CCD in timing mode discovered X-ray pulsations with a period of 3.93 ms and an orbit of 11 hr (Fig. 13), exactly matching the timing parameters of PSR J1824-2452I, a previously known radio pulsar in the cluster, and proving that the transient LMXB and the radio MSP were the same object. When accreting material penetrates within the light cylinder of the radio pulsar and falls onto the polar caps, it quenches the radio pulsation mechanism and replaces it with X-ray pulsations.

radio pulsations from another binary MSP, the 1.69 ms PSR J1023+0038, were observed to turn off for the first time since their detection in 2007, indicating that it has probably started accreting. There had been evidence that this 4.8 hr binary was accreting in 2000-2001, when optical emission lines and the blue continuum characteristic of an accretion disk were seen. Now accretion has resumed, as evidenced by enhanced optical and X-ray emission observed after the radio pulsations turned off. With a flux of $1 \times 10^{-11} \text{ erg cm}^{-2} \text{ s}^{-1}$, the 0.3–10 keV X-rays from PSR J1023+0038 were not quite bright enough to trigger any all-sky monitor, but an entire XMM revolution was used to observe it in October 2013 (PI: Bogdanov).

This observation will enable X-ray pulsations to be detected, if they are present, as in PSR J1824-2452I. Variable emission from the accretion disk, and orbital modulation in the optical due to heating of the illuminated face of the companion star will also be studied. PSR J1023+0038 was previously observed by XMM in its quiescent radio pulsar state (Archibald et al. 2010), which revealed X-ray emission modulated on the orbital period with a maximum at superior conjunction of the companion star, demonstrating the existence of the predicted intrabinary shock between the pulsar wind and the ablated face of the companion. Now an accretion disk has formed, which is increasing the pressure of the pulsar wind close to the NS. This is evident from rapid X-ray fluctuations, and enhanced Fermi gamma-ray flux coming from a now more luminous shock.

Both PSR J1023+0038 and IGR J18245-2452 are nearly Roche-lobe-filling systems called “redbacks,” which are related to the black-widow pulsars, the energetic MSPs that have nearly evaporated their companion stars. These and other eclipsing millisecond pulsars that were once rare are being found in large numbers by Fermi and are the subject of detailed X-ray study by XMM (e.g., Bogdanov et al. 2013). With its long orbit, 30 ms timing, and high throughput, XMM is uniquely suited to studying the rich X-ray behavior of these complex systems, which display rapid variability while in the accreting state. The OM enables complete coverage of binary orbits, which is often not possible from the ground because of seasonal restrictions and Earth’s rotation.

Synchronous X-ray and Radio Mode Switches: A Rapid Global Transformation of the Pulsar Magnetosphere [PSR B0943+10]

(Hermsen et al. 2013)

and

Simultaneous XMM-Newton Radio Observations of the Mode-switching Radio Pulsar PSR B1822-09

(Hermsen et al. 2018)

New phenomenology discovered using XMM — coordinated radio/X-ray mode-switching

Changes in radio emission behavior have been well documented for a number of pulsars,

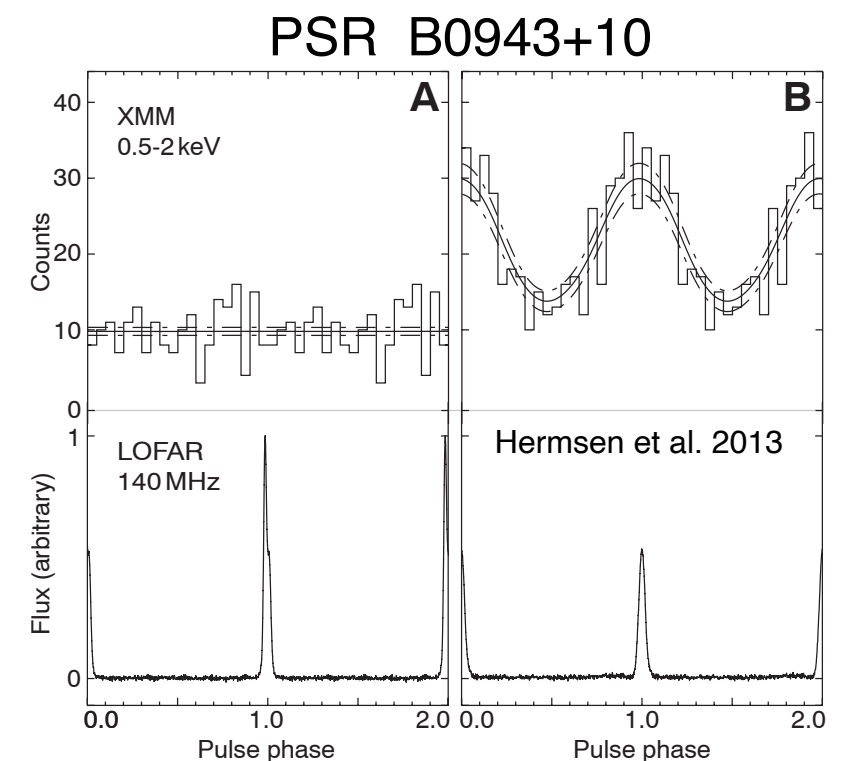
These manifest as switches between ordered and disordered variations in intensity and pulse shapes,

Coordinated radio and X-ray observations now reveal coordinated state change between then two bands,

Radio-“quiet” mode / 100% pulsed thermal emission,

Radio-“bright” mode / unpulsed, nonthermal X-rays,

This new behavior points to a global change in the pulsar magnetosphere, possibly related to local ISM accretion.



NuSTAR Hard X-Ray Observations of the Energetic MSP PSR B1821-24, PSR B1937+21, and PSR J0218+4232

(Gotthelf & Bogdanov 2017)

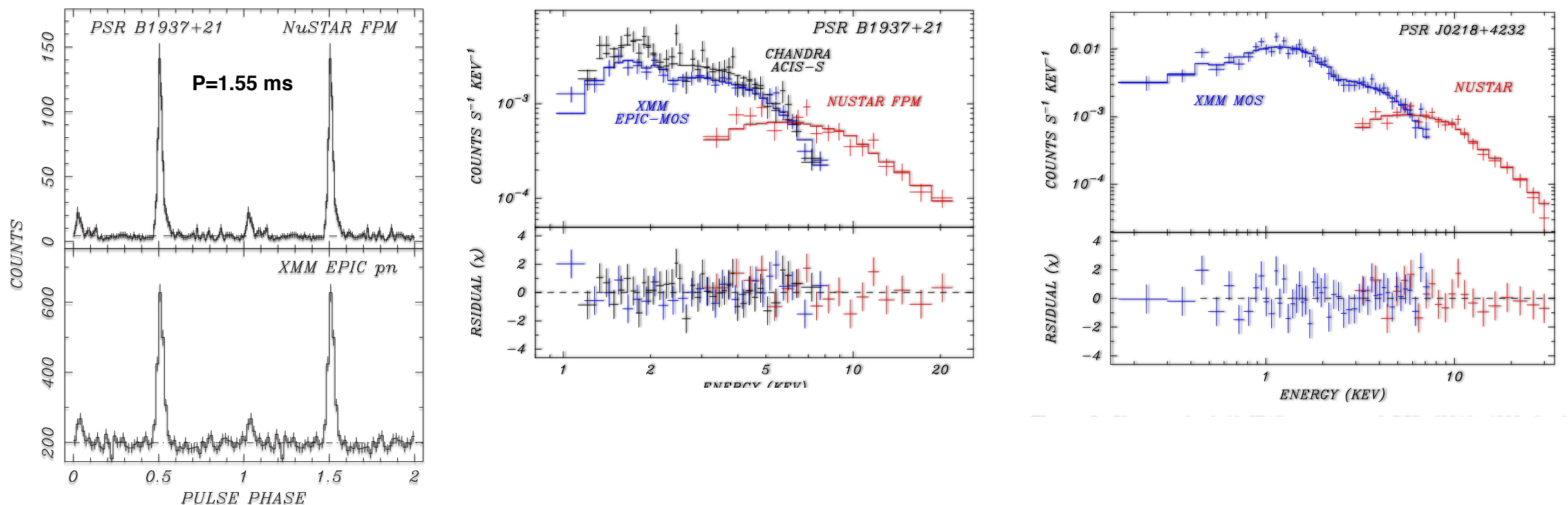
Examples of Joint XMM-NuSTAR Broad-band Spectroscopy

Phase-resolved spectroscopy in the 0.5–79 keV range for all three objects,

Best measurements of their broadband spectra and pulsed emission to-date,

No conclusive evidence for a spectral turnover or break.

Turnover required in the 100 keV to 100 MeV range to march up Fermi γ -ray emission



XMM 20th Highlights: The MSP

XMM Observations of CCO Anti-magnetars

CCO Pulsar	SNR	XMM (ks)
1E 1207.4-5209	PKS 1209-51/52	974
PSR J0821-4300	Puppis A	806
PSR J1852+0040	Kes 79	525
	3 Total:	2,305

Central Compact Objects in Supernova Remnants

CCO	SNR	Age (kyr)	d (kpc)	P (ms)	f_p^a (%)	B_s (10^{10} G)	$L_{x,\text{bol}}$ (erg s $^{-1}$)
RX J0822.0–4300	Puppis A	4.5	2.2	112	11	2.9	5.6×10^{33}
1E 1207.4–5209	PKS 1209–51/52	7	2.2	424	9	9.8	2.5×10^{33}
CXOU J185238.6+004020	Kes 79	7	7	105	64	3.1	5.3×10^{33}
CXOU J085201.4–461753	G266.1–1.2	1	1	...	< 7	...	2.5×10^{32}
CXOU J160103.1–513353	G330.2+1.0	$\gtrsim 3$	5	...	< 40	...	1.5×10^{33}
1WGA J1713.4–3949	G347.3–0.5	1.6	1.3	...	< 7	...	$\sim 1 \times 10^{33}$
XMMU J172054.5–372652	G350.1–0.3	0.9	4.5	3.9×10^{33}
CXOU J232327.9+584842	Cas A	0.33	3.4	...	< 12	...	4.7×10^{33}
2XMMi J115836.1–623516	G296.8–0.3	10	9.6	1.1×10^{33}
XMMU J173203.3–344518	G353.6–0.7	~ 27	3.2	...	< 9	...	1.3×10^{34}
CXOU J181852.0–150213	G15.9+0.2	1 – 3	(8.5)	$\sim 1 \times 10^{33}$

Note — Above the line are eight well-established CCOs. Below the line are three candidates. Upper limits on pulsed fraction are for a search down to $P = 12$ ms or smaller.

Three CCOs are pulsars (Anti-magnetars)

Two discovered by XMM, and one correctly timed by XMM.

Defines a new class of NSs - likely explains properties of the other CCOs.

Deep XMM searches of the others - Uniform surface? Unfavorable beaming?

A Mystery: 1E 1207.4-5209 Timing Results

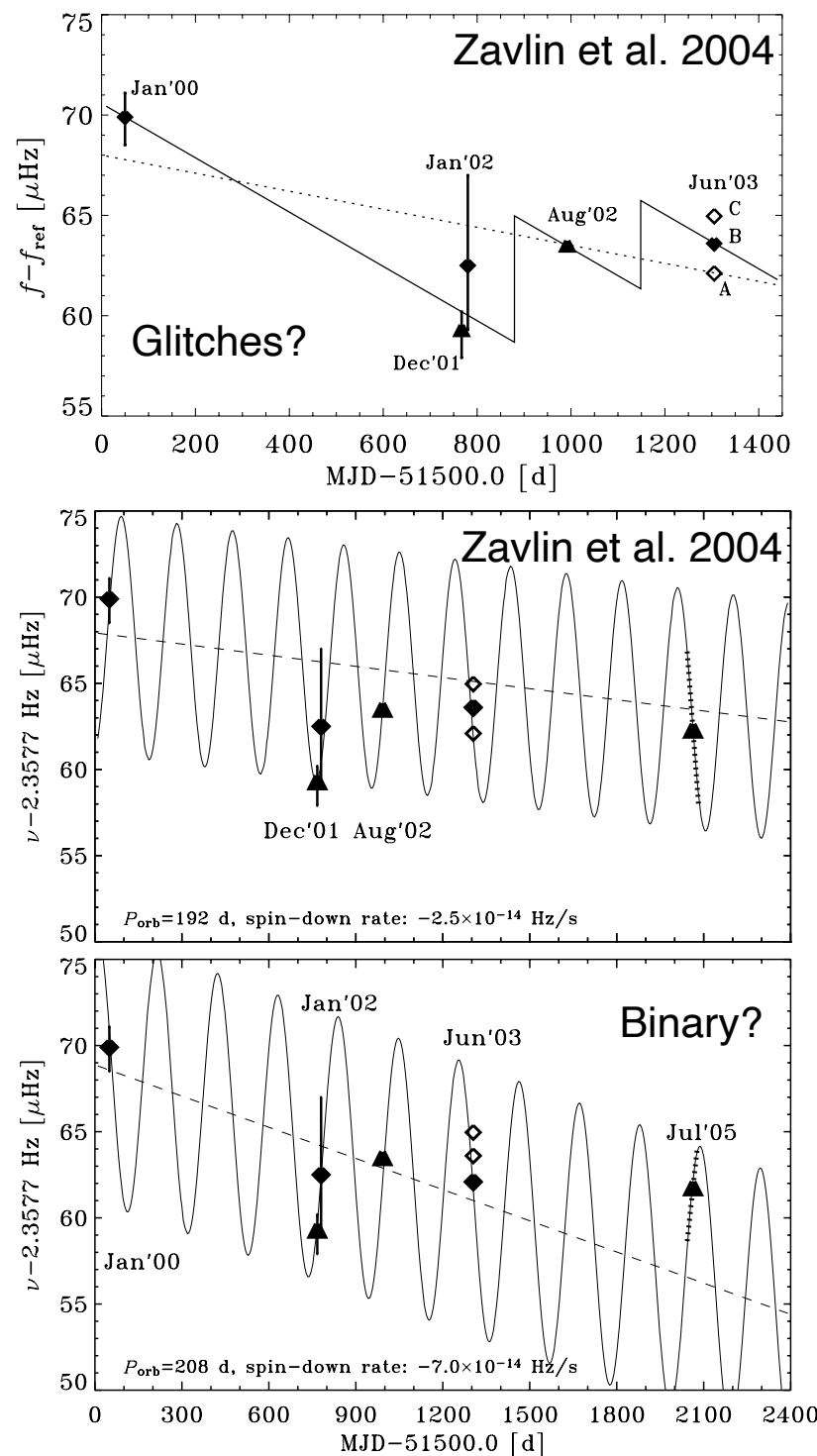
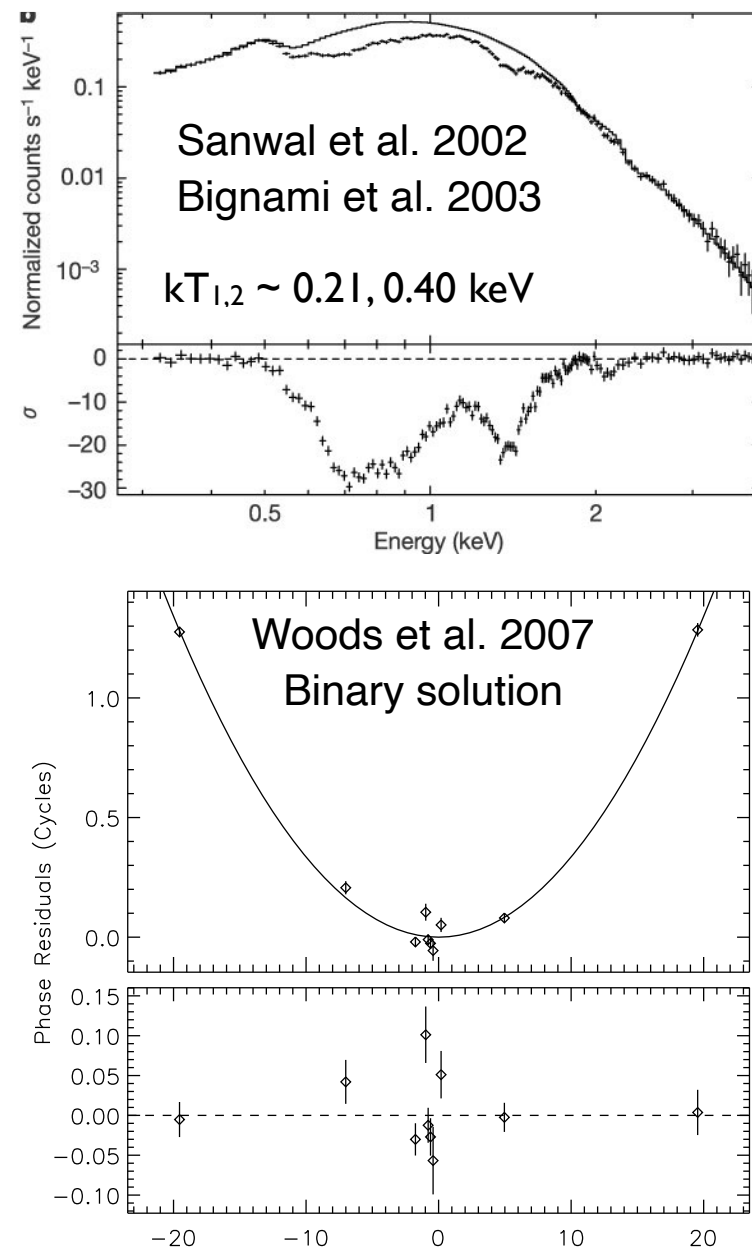


Fig. 4 Candidate orbital solutions for 1E1207 consistent with our MOD2 (*top*) timing solution and MOD1 (*bottom*) timing solution



- 424 ms pulsar in PKS 1209-52 (Zavin et al. 2000),
- 5 yr X-ray timing data
- Analyzed by 4 different groups, 7 major papers,
- Contradictory reports of large amplitude glitches, spin-up, and spin-down?
- B-field incompatible with spectral results, too large,
- Unlike any other pulsar and difficult to explain!

Pavlov et al 2002: $\dot{P} = (0.7-3) \times 10^{-14}$

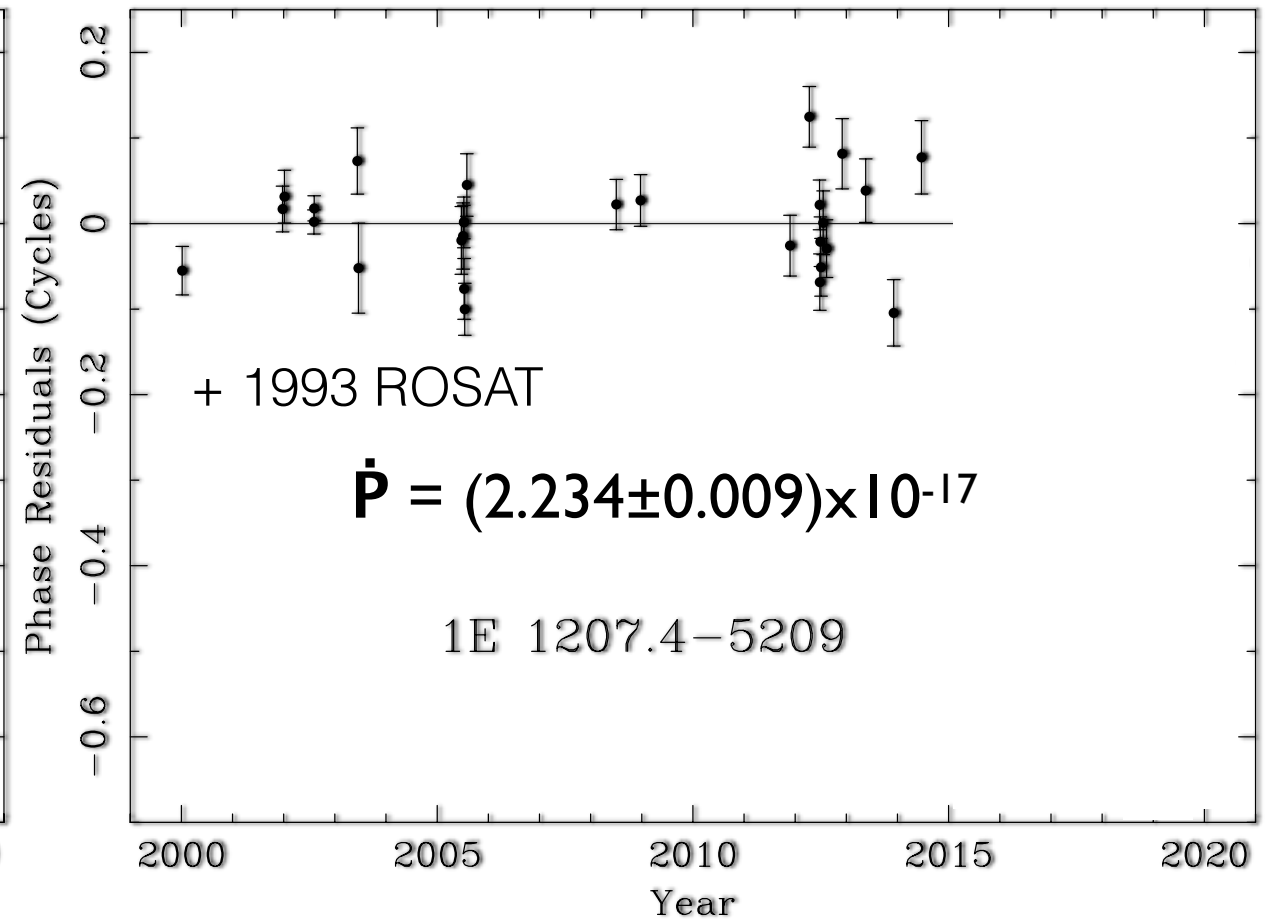
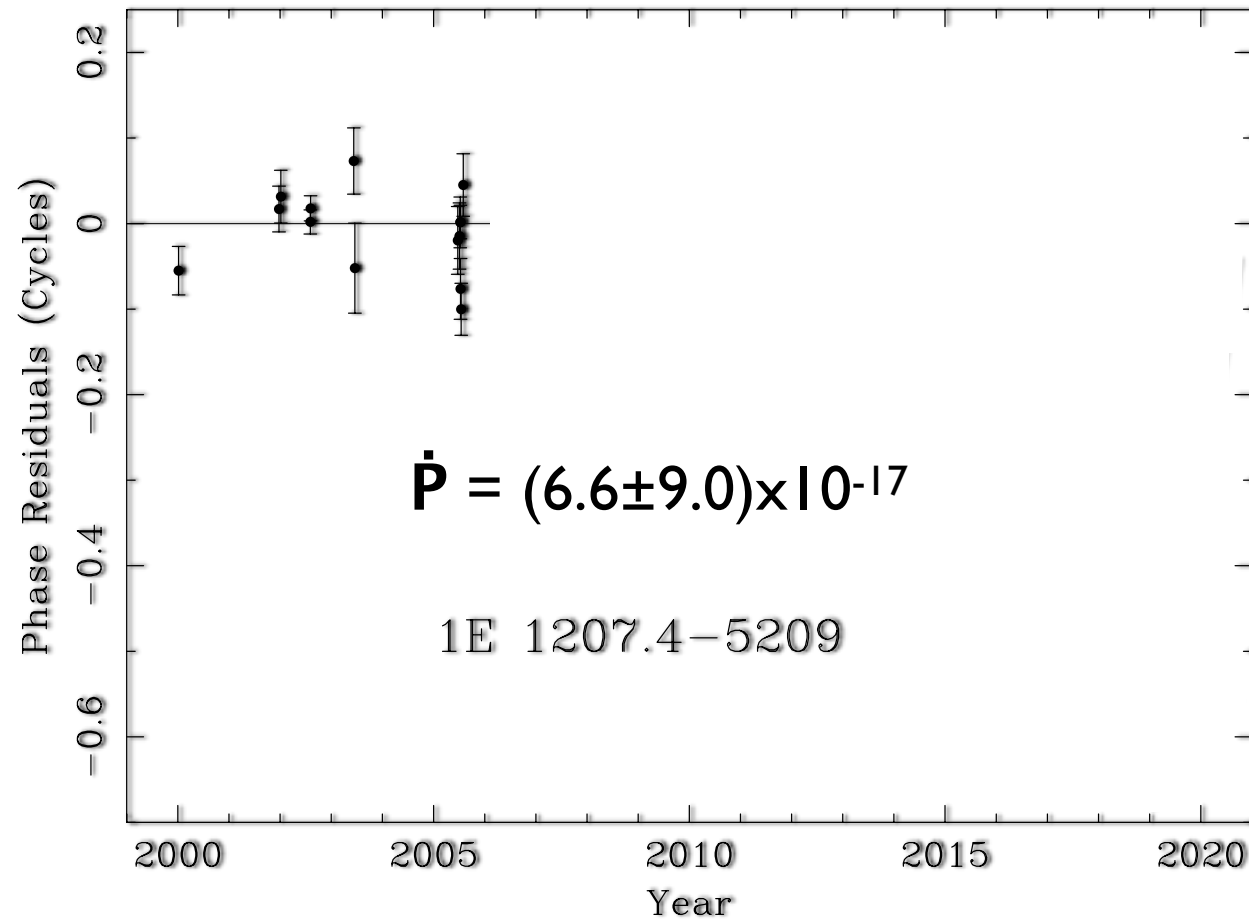
Mereghetti et al. 2002: $\dot{P} = (1.98 \pm 0.83) \times 10^{-14}$

De Luca et al. 2004; $\dot{P} = (1.4 \pm 0.3) \times 10^{-14}$

Precise Timing of the X-ray Pulsar 1E 1207.4-5209: A Steady Neutron Star Weakly Magnetized at Birth

Gotthelf & Halpern (2007)

After correcting for XMM time jumps — no measurable spin-down in 5 yrs !

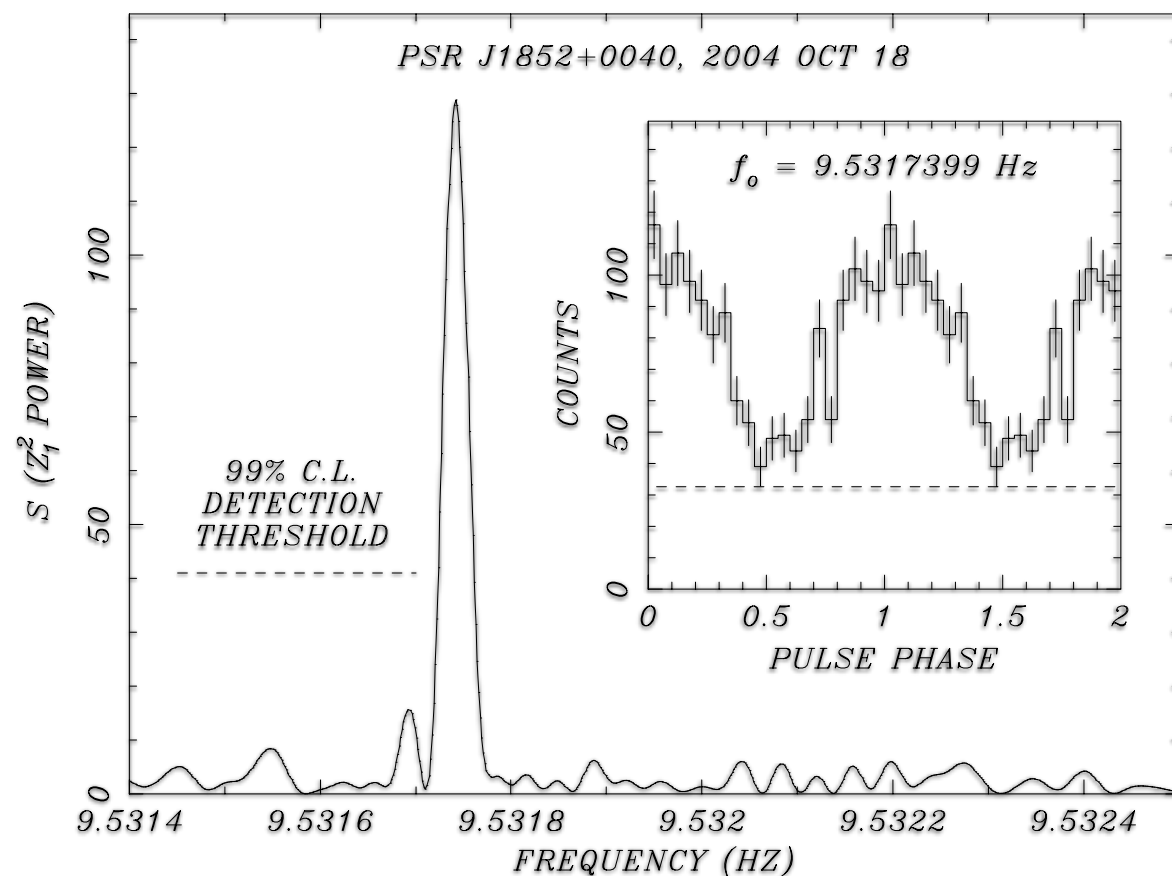


Discovery of a 105 ms X-Ray Pulsar in Kesteven 79: On the Nature of Compact Central Objects in Supernova Remnants

Gotthelf, Halpern & Seward (2005)

- Central source in Kes 79 resolved by Chandra (Seward et al. 2003)
- Location, spectrum, and flux, etc... consistent with a CCO
- Steady flux, deep radio and optical limits

A second CCO pulsar, $P = 105$ ms, detected with XMM



2004 - 2007 XMM Observations:

No measurable change in period in 3 yrs.

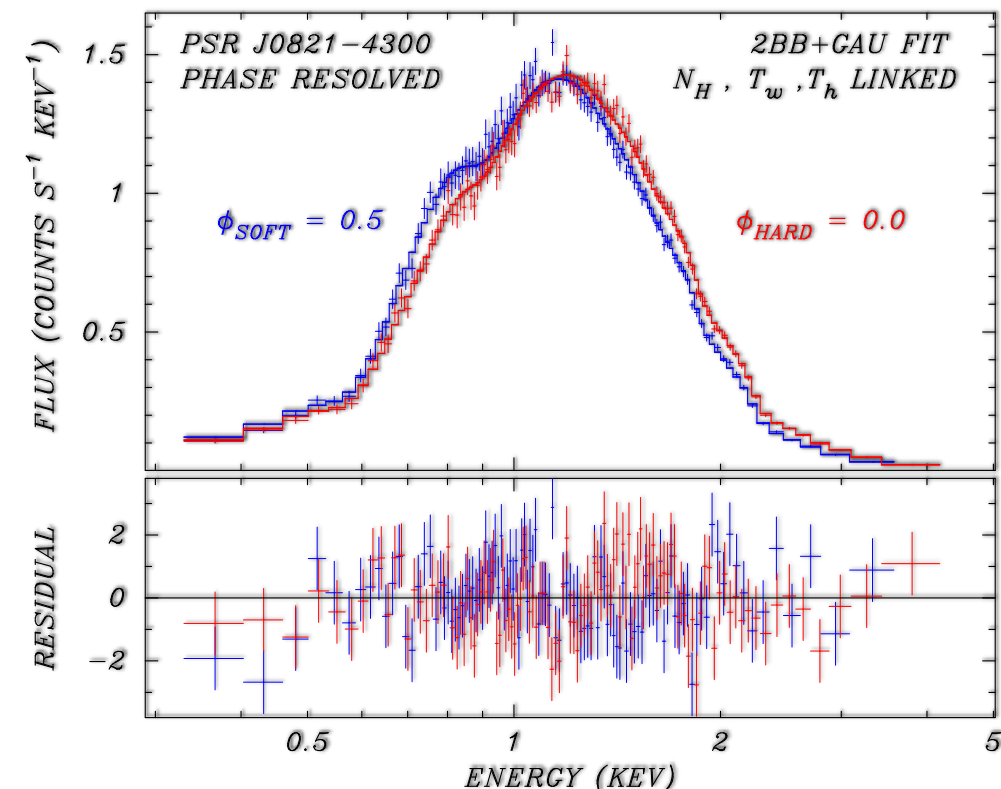
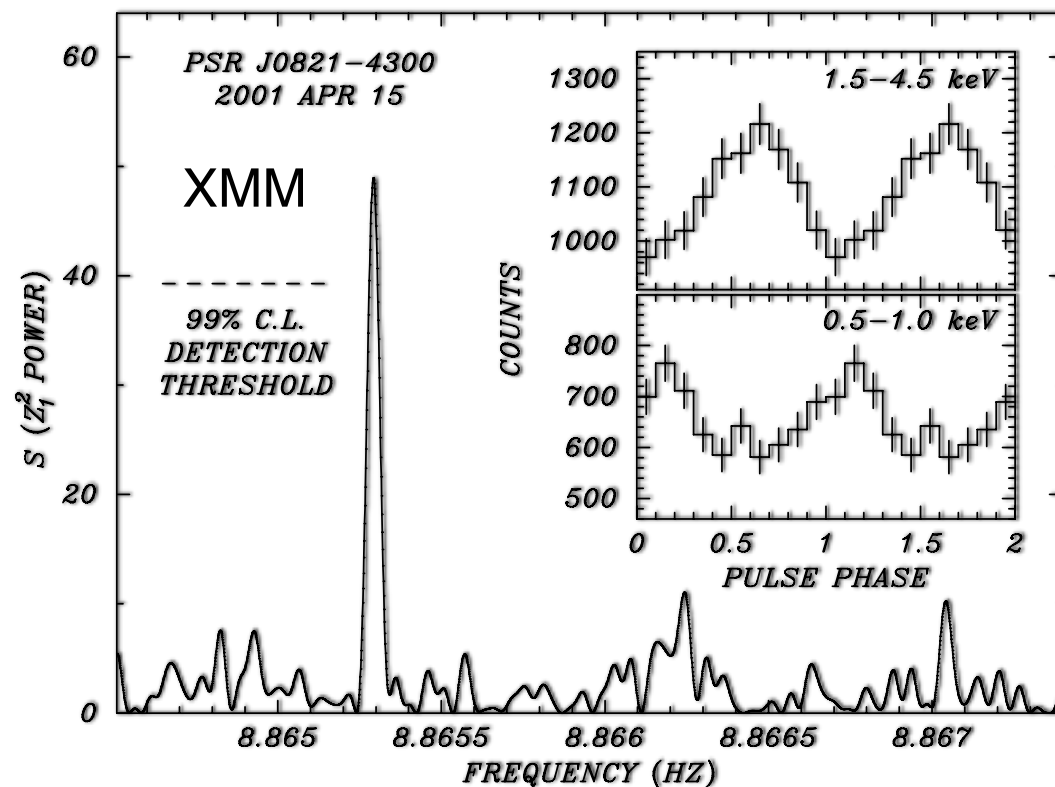
Weak inferred B-field, but highly modulated,

Again, unprecedented for a young PSR!

Discovery of a 112 ms X-Ray Pulsar in Puppis A: Further Evidence of Neutron Stars Weakly Magnetized at Birth

Gotthelf & Halpern (2007)

PSR J0821–4300: The remarkable phase-shifting 112 ms CCO pulsar



Found in 6 yr old archival XMM data, previously searched.

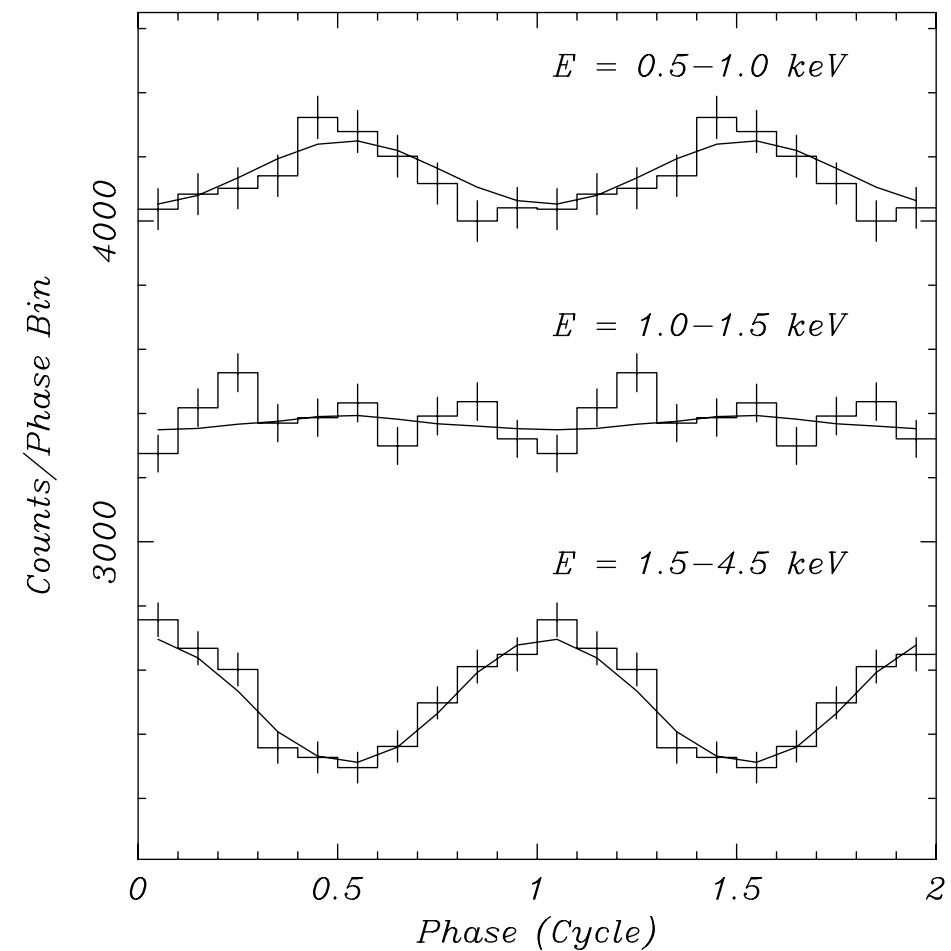
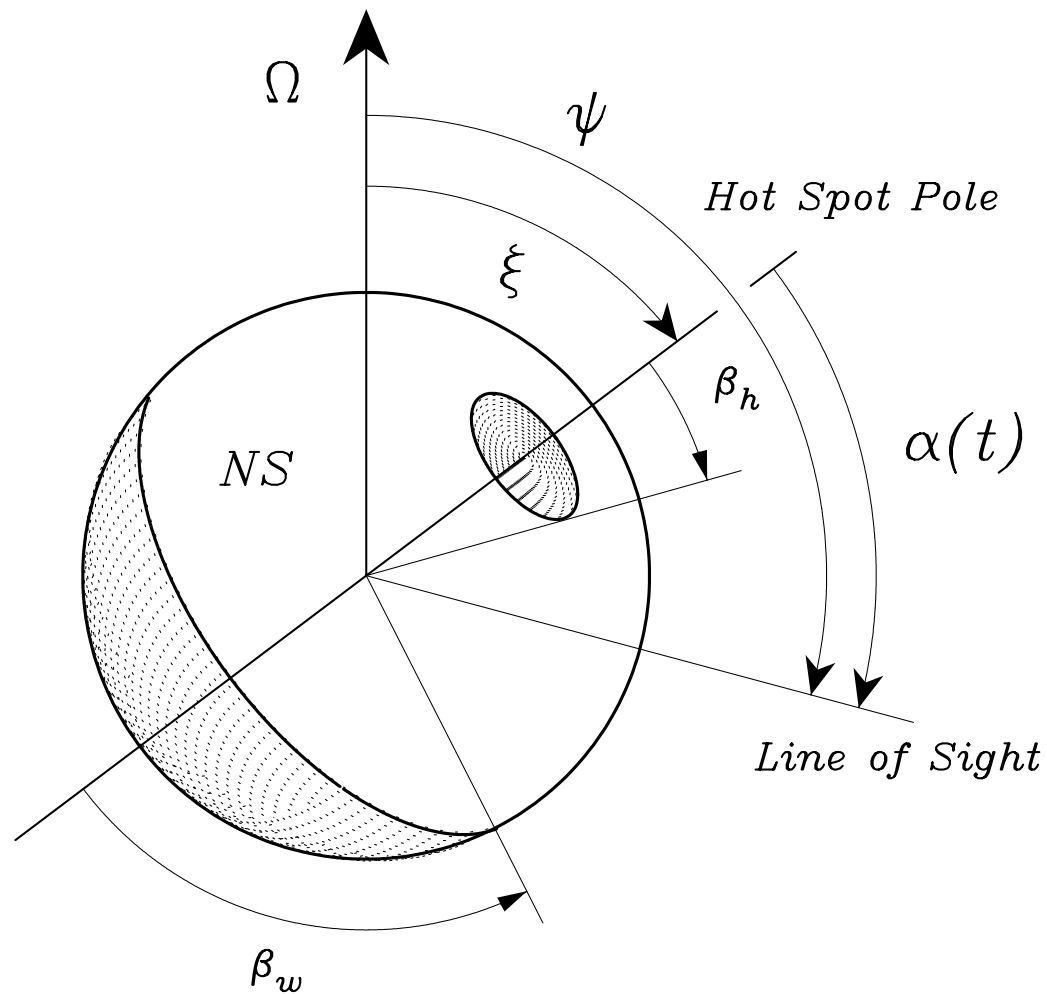
Two observations separated by 6 month,

Required trial energy & aperture cuts & comparing marginal signal between observations

Antipodal Model: A Numerical Simulation

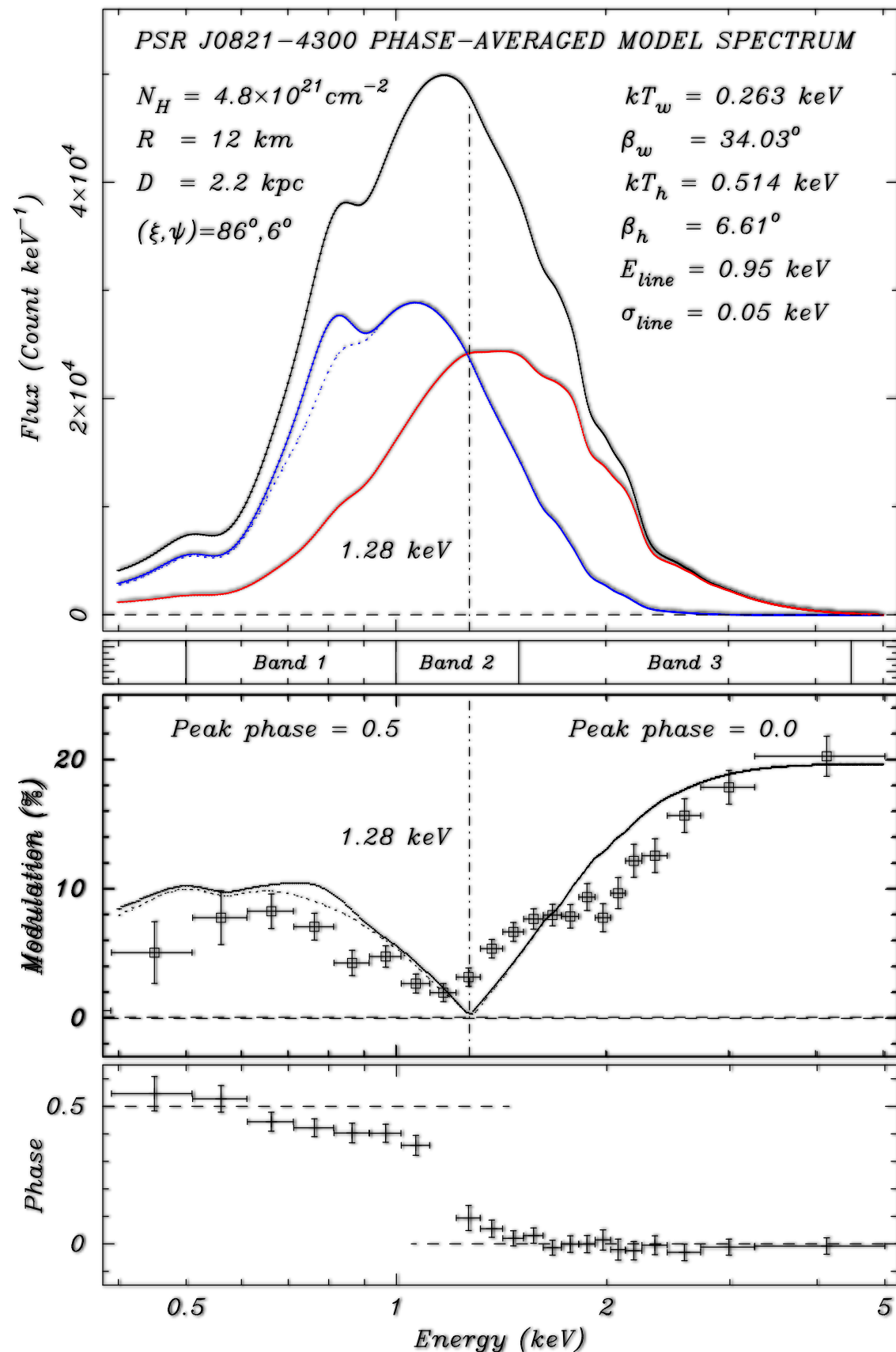
(Gotthelf, Perna, & Halpern 2010)

Two antipodal emission spots of size $\beta_{h,w}$ and BB Temp. $T_{h,w}$
XSPEC model spectral fits, assumed N_H , Distance, NS Radius

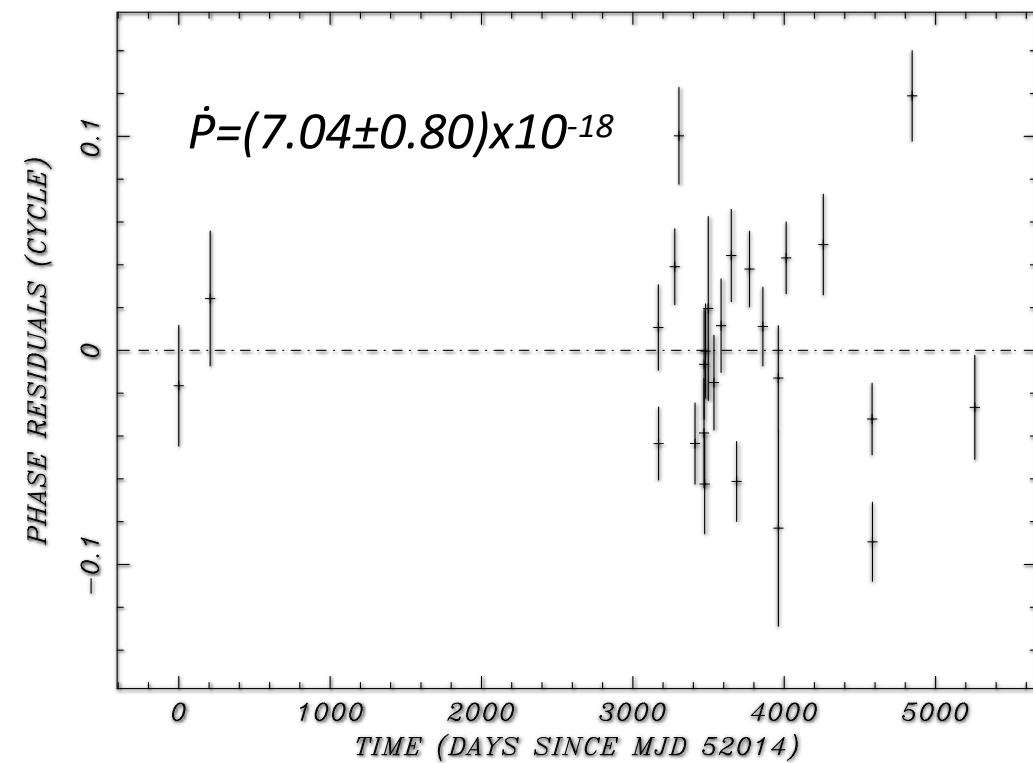


Find (ξ, ψ) that can reproduce modulation and phase reversal of energy-dependent pulse profile in three interesting energy bands.

Current, 800 ks of XMM data



14 yrs phase-coherent ephemeris



Sufficient photons to fully resolve modulations vs. energy

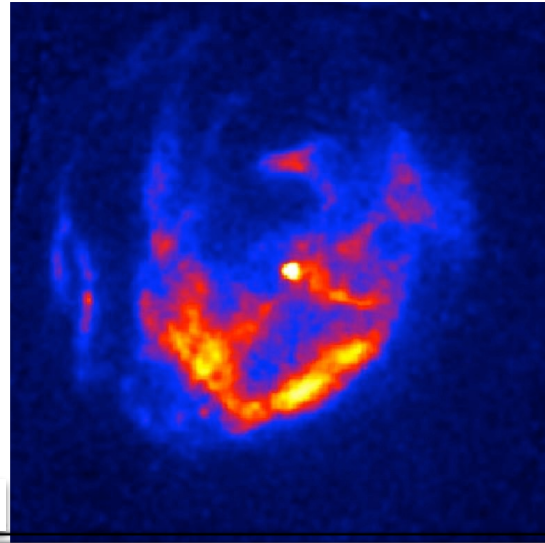
*Interesting structure - offset dipole?
anisotropic temp distribution?*

$$f_p(E) = \frac{f_1 F_1(E) \sin[\psi(E)] + f_2 F_2(E) \sin[\psi(E) + \Delta\phi]}{F_1(E) + F_2(E)},$$

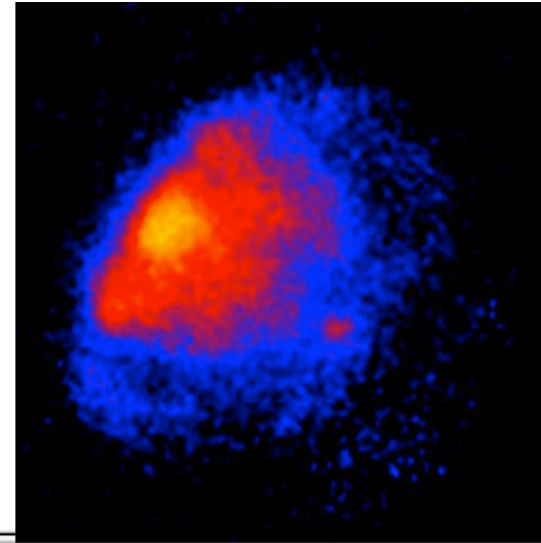
$$\psi(E) = \tan^{-1} \left[\frac{\frac{f_1 F_1(E)}{f_2 F_2(E)} + \cos(\Delta\phi)}{\sin(\Delta\phi)} \right]$$

Timing Properties of Anti-magnetars

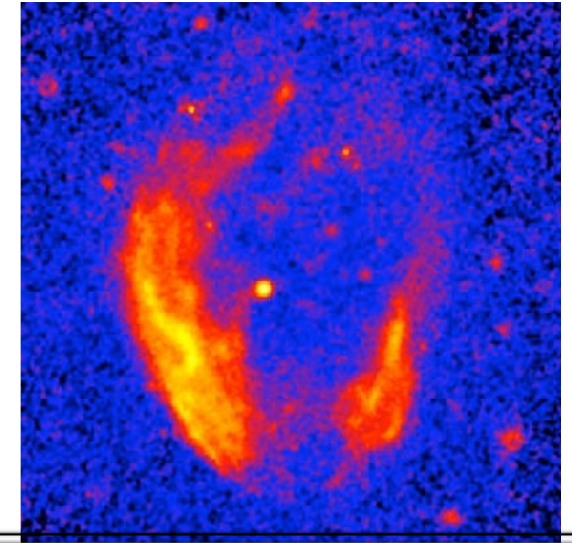
Complete Timing
Results on
Known
Anti-magnetars



PSR J1852+0040
SNR Kes 79

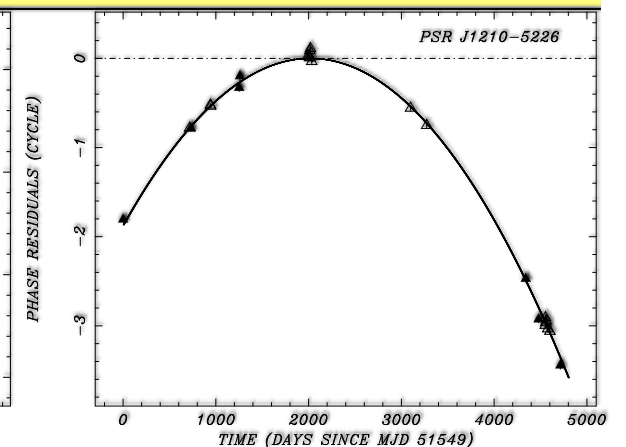
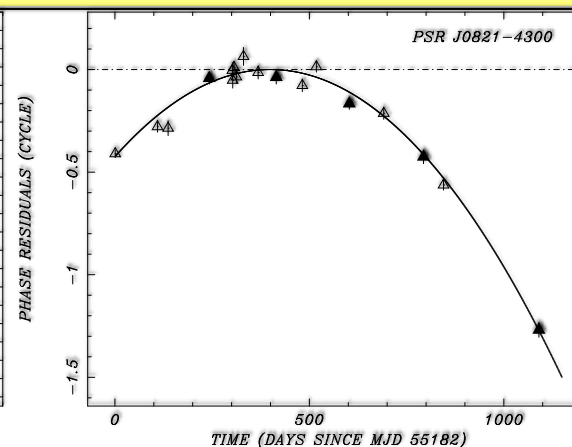
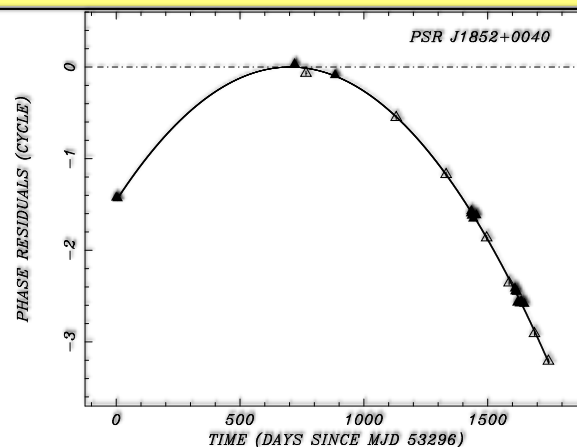


PSR J0821-4300
SNR Puppis A



PSR J1210-5209
SNR PKS 1209-52/52

P (ms)	104.9126	112.7995	424.1307
$\dot{P}(\times 10^{-17})^a$	0.868 ± 0.009	0.704 ± 0.80	2.234 ± 0.009
Pulsed Fraction (%)	64	11	9
$\dot{E} \equiv I\Omega\dot{\Omega}$ (erg s ⁻¹)	3.0×10^{32}	1.9×10^{32}	1.2×10^{31}
$L(\text{bol})/\dot{E}^b$	18	31	167
$B_p(\times 10^{10}$ G)	3.1	2.9	9.8
$\tau \equiv P/2\dot{P}$ (Myr)	192	254	302
SNR age (kyr)	~ 7	~ 4	~ 7



XMM 20th Highlights: The CCO Pulsars

The Mysteries of the CCO Pulsars (Anti-magnetars)

- Slow spin-down imply 200 Myr, incompatible with SNR age,
- High X-ray luminosity incompatible with spin-down power,
- Similar spectrum to magnetars, but 10^4 times weaker B-fields,
- Weak B-field incompatible w/ highly modulated signal of Kes 79.
- Large absorption features in spectrum of 1E 1207.4-5209 ?
- Variable absorption features of Puppis A CCO ?

Hypothesis - buried magnetar-strength toroidal field generating hot spots.

The First Glitch in a Central Compact Object Pulsar: 1E 1207.4-5209

Gotthelf & Halpern (2018)

Glitch from an otherwise extremely stable rotator, $\Delta f/f < (2.8 \pm 0.4) \times 10^{-9}$

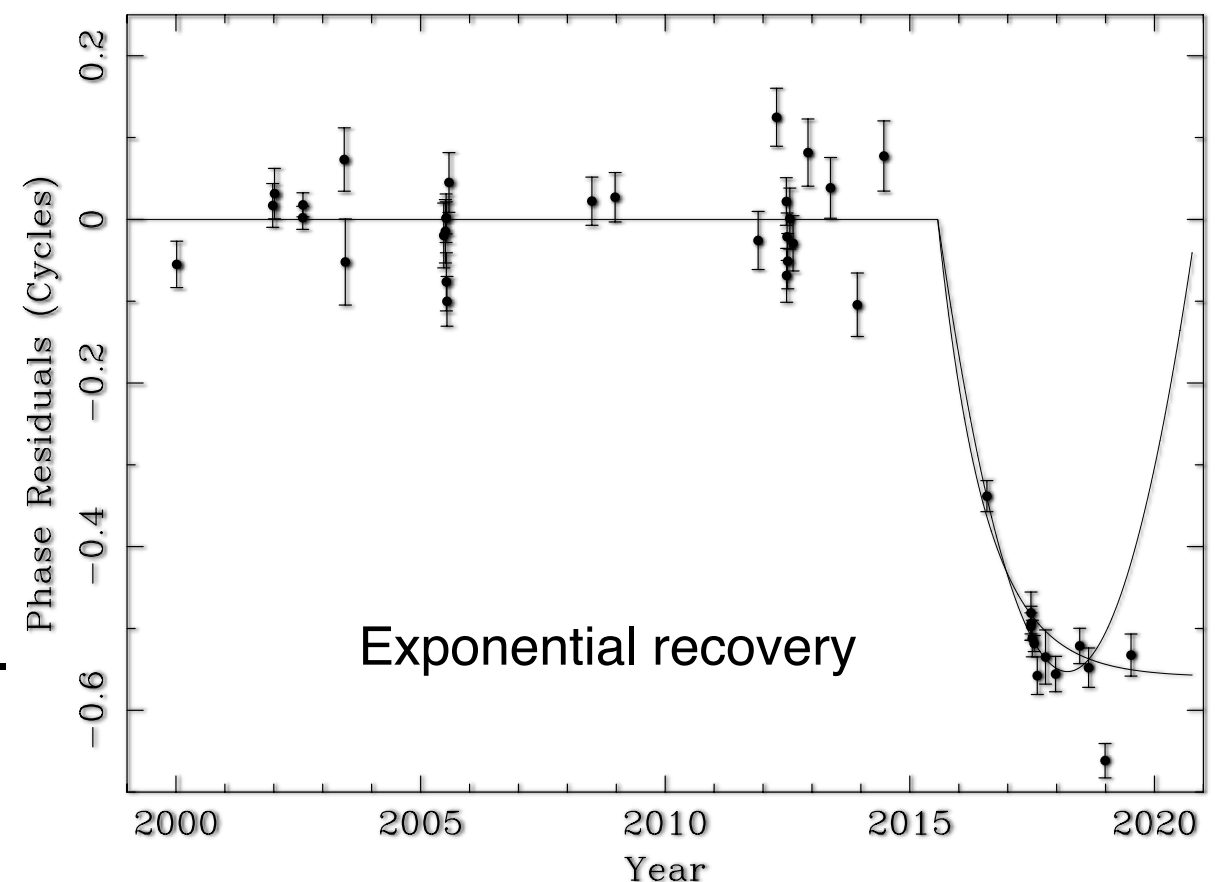
Most unusual:

- Although magnitude typical of a pulsar,
- Old pulsars with \dot{f} this small never glitch,
- And no large increase in \dot{f} ,
- No change in line features, no disruption in the dipole field due to or result of glitch.

Hypothesis:

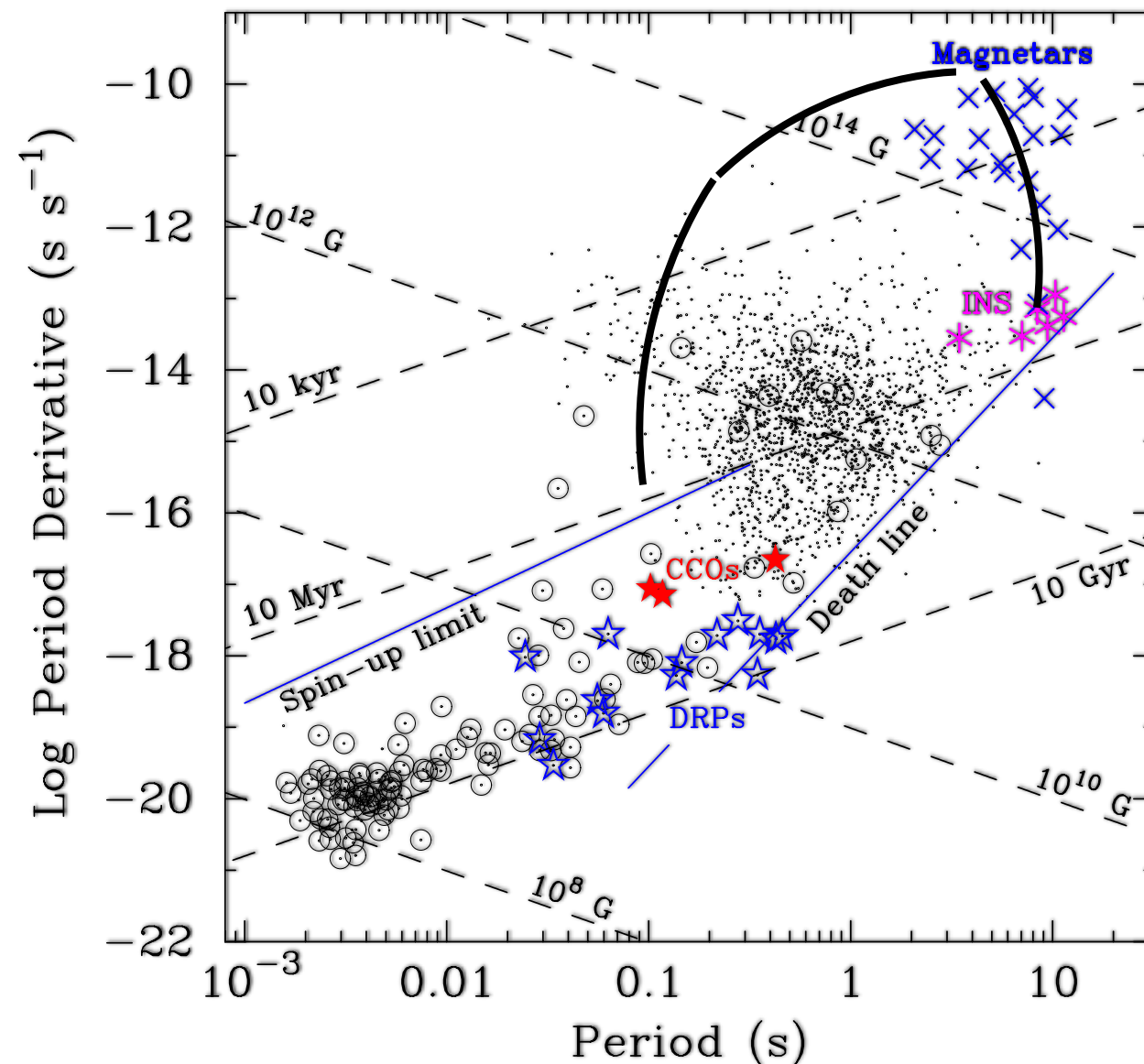
- CCOs theorized to have buried magnetar-strength fields that diffuse out in < 1 Myr ,
- These result from prompt burial of B-field due to fallback of supernova ejecta,
- Glitch are triggered by diffusion of these strong fields,
- These strong internal toroidal field generate the hot spots.

New XMM / NICER timing program underway!



Magnetic Evolution for NSs ?

CCO -> Magnetar -> INS ?



Pulsar Evolution =
Magnetic Field Evolution!!!

